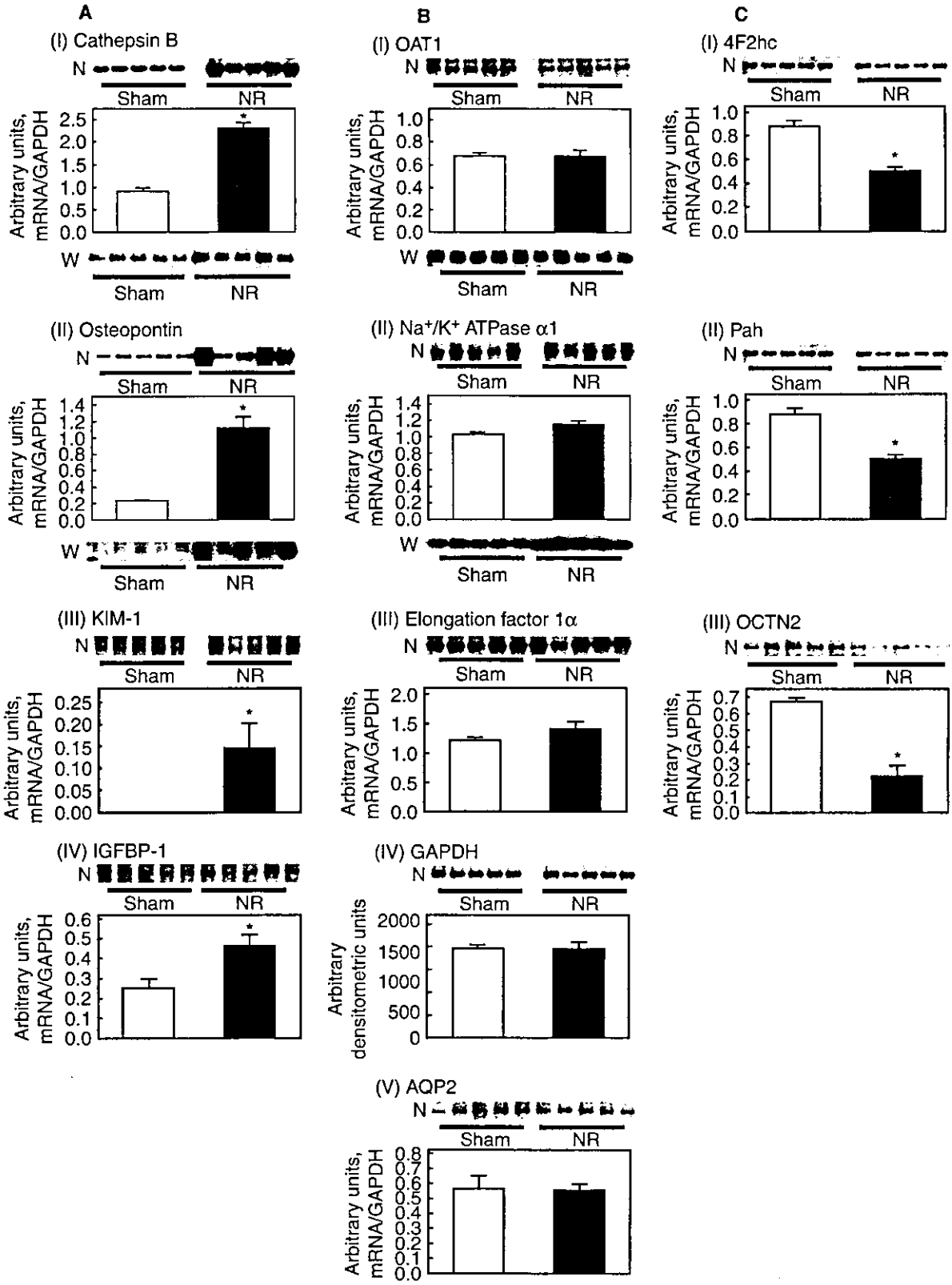

Fig. 1. Northern blotting or Western blotting of the genes up-regulated (*A*), maintained (*B*), or down-regulated (*C*) in the 5/6 nephrectomized (NR) kidney in the subtractive database. Five micrograms of total RNA of kidneys was hybridized with each probe under high stringency conditions. The protein expressions of cathepsin B, osteopontin, OAT1, and Na^+-K^+ ATPase α1 subunit, whose antibodies were available, were also examined by Western blotting. The amounts of mRNA were quantified by densitometry and normalized to glyceraldehyde-3-phosphate dehydrogenase (GAPDH). Each column represents the mean ± SEM of five rats. $^*P < 0.05$, significantly different from sham (Student unpaired *t* test). Abbreviations are: N, Northern blotting; W, Western blotting; KIM-1, kidney injury molecule-1; IGFBP-1, insulin like growth factor binding protein-1; OAT1, organic anion transporter1; AQP2, aquaporin 2; Pah, phenylalanine hydroxylase; OCTN2, novel organic cation transporter 2.

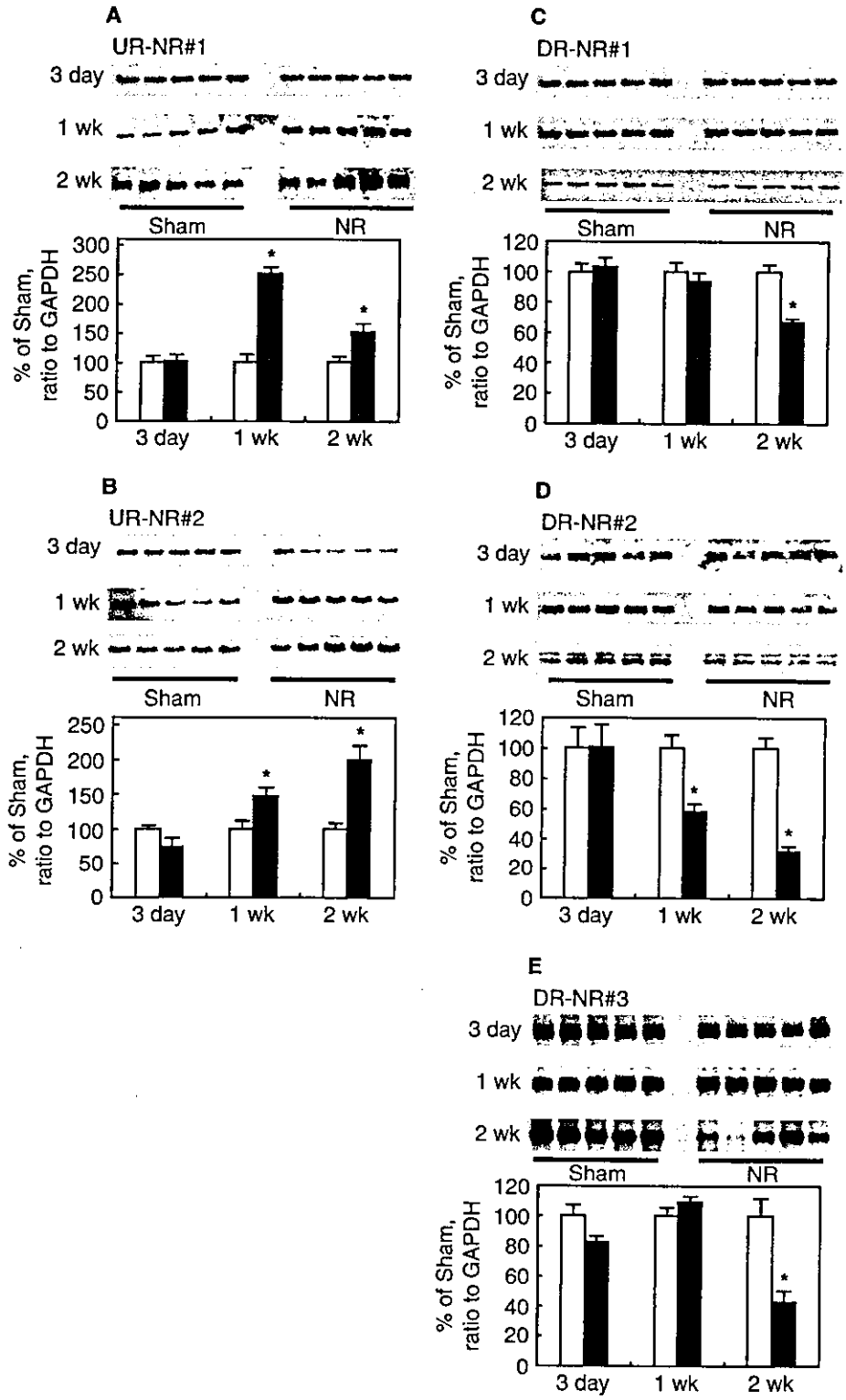

Fig. 2. Northern blotting of the five unknown genes in the 5/6 nephrectomized (NR) and sham-operated (sham) kidneys. mRNA expression of up-regulated 5/6 nephrectomized (UR-NR) #1 (*A*), UR-NR #2 (*B*), down-regulated 5/6 nephrectomized (DR-NR) #1 (*C*), DR-NR #2 (*D*), and DR-NR #3 (*E*) in the 5/6 nephrectomized and sham-operated kidneys 3 days, 1 week, and 2 weeks after the operation was examined. Five micrograms of total RNA of kidneys was hybridized with each probe under high stringency conditions. The amounts of mRNA were quantified by densitometry and normalized to glyceraldehyde-3-phosphate dehydrogenase (GAPDH). Each column represents the mean ± SEM of five rats. $^*P < 0.05$, significantly different from sham-operated (Student unpaired *t* test).

Table 5. State of renal function of the 5/6 nephrectomized (NR) and sham-operated (sham) rats 3 days, 1 week, and 2 weeks after subtotal nephrectomy

		Body weight *g*	Plasma creatinine *mg/dL*	Blood urea nitrogen *mg/dL*	Creatinine clearance *mL/min/kg*	Urinary excretion of albumin *mg/day*	Urinary excretion of NAG *U/day*	Kidney weight *g*
Sham	3 days	204 ± 2	0.4 ± 0.0	14 ± 0	7.0 ± 0.5	0.2 ± 0.0	156 ± 15	1.6 ± 0.0
	1 week	232 ± 3	0.5 ± 0.0	11 ± 0	5.1 ± 0.4	0.4 ± 0.1	232 ± 19	1.7 ± 0.0
	2 weeks	270 ± 4	0.5 ± 0.0	14 ± 2	5.2 ± 0.1	0.3 ± 0.1	211 ± 16	1.7 ± 0.0
NR	3 days	188 ± 3[a]	1.4 ± 0.1[a]	56 ± 2[a]	2.1 ± 0.3[a]	6.9 ± 1.7[a]	180 ± 44	0.3 ± 0.0[a]
	1 week	192 ± 5[a]	1.1 ± 0.1[a]	48 ± 2[a]	2.1 ± 0.1[a]	7.1 ± 2.2[a]	177 ± 15	0.4 ± 0.0[a]
	2 weeks	230 ± 10[a]	1.2 ± 0.1[a]	59 ± 6[a]	1.9 ± 0.1[a]	4.0 ± 2.2[a]	187 ± 11	0.6 ± 0.0[a]

NAG is *N*-acetyl-β-D-glucosaminidase.
The urine and blood samples were collected at 3 days, 1 week, and 2 weeks after the operation. Data represent the mean ± SEM of five rats.
[a] $P < 0.05$, significantly different from sham (Student unpaired *t* test).

nephropathy. The mRNA expression of DR-NR #2 and #3 was significantly decreased in the cisplatin, but not the vancomycin nephropathy. There were no changes in the mRNA expression of UR-NR #2 and DR-NR #1 among the three treated groups.

Structure of unknown genes

UR-NR #1, UR-NR #2, DR-NR #1, DR-NR #2, and DR-NR #3 were fully isolated by the 5′ RACE technique. They were all highly homologous to the mouse or human putative clone in which only nucleic acid sequences were identified. Their deduced amino acid sequences were also highly homologous to the putative proteins corresponding to the putative nucleotide (Table 7). Figure 6 shows their deduced amino acid sequences, and the conserved domains are listed in Table 8. The topologies of these five proteins were predicted by SOSUI system, which is a tool for secondary structure prediction of membrane proteins (*www.sosui.proteome.bio.taut.ac.jp*, Mitaku and Hirokawa, 1999). DR-NR #3 was found to be a membrane-bound protein. DR-NR #1 was predicted to be a secreted protein, but the other three proteins were thought to be soluble proteins. UR-NR #1 consisted of 1075 bp nucleotides, and contained an open reading frame of 117 amino acids. UR-NR #1 did not show any significant similarity with known genes and conserved domains (Fig. 6A). UR-NR #2 consisted of 3752 bp nucleotides, and contained an open reading frame of 353 amino acids. A conserved domain search revealed that UR-NR #2 had a Tre/Bub2/Cdc16 (TBC) domain, which was the guanosine triphosphatase (GTPase) activator protein of Rab-like small GTPases (Rab-GAPs), regulators of intracellular vesicle trafficking (Fig. 6B) [27]. DR-NR #1 consisted of 3315 bp nucleotides, contained an open reading frame of 297 amino acids, and had a conserved domain of isochorismatase, a family of hydrolase enzymes (Fig. 6C) [28]. DR-NR #2 consisted of 3032 bp nucleotides, and contained an open reading frame of 596 amino acids (Fig. 6D). DR-NR #2 had a conserved domain of Rho-GAPs, which negatively regulated Rho [29, 30]. DR-NR #3 consisted of 1753 bp nucleotides, and contained an open reading frame of 324 amino acids (Fig. 6E). DR-NR #3 contained a typical $NADP^+$-binding motif (TGxxxGxG) and a short chain dehydrogenase active site motif (S-Y-K) [31]. In addition, 101 amino acids of DR-NR #3, from 89 to 189, were very similar to "hypertension-induced rat S2 protein," which was previously reported to be up-regulated in spontaneously hypertensive rats [32]. The similarity was approximately 98% in the matched region, totaling 31% homology (Fig. 6E). Therefore, DR-NR #3 would be a full length of rat S2 protein.

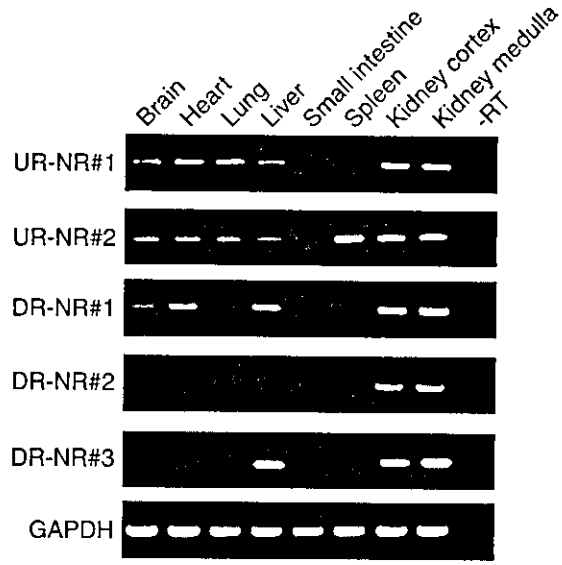

Fig. 3. Detection of mRNA of the five unknown genes in rat tissues by reverse transcription-polymerase chain reaction (RT-PCR). Total RNA (5 μg) from the tissues indicated was reverse-transcribed, and the cDNA synthesized was amplified using a set of primers specific for each clone. The PCR products were separated by electrophoresis through 1% agarose gels and stained with ethidium bromide. Abbreviations are: −RT, whole kidney without reverse transcriptase; UR-NR #1, up-regulated 5/6 nephrectomized #1; UR-NR #2, up-regulated 5/6 nephrectomized #2; DR-NR #1, down-regulated 5/6 nephrectomized #1; DR-NR #2, down-regulated 5/6 nephrectomized #2; DR-NR #3, down-regulated 5/6 nephrectomized #3; GADPH, glyceraldehyde-3-phosphate dehydrogenase.

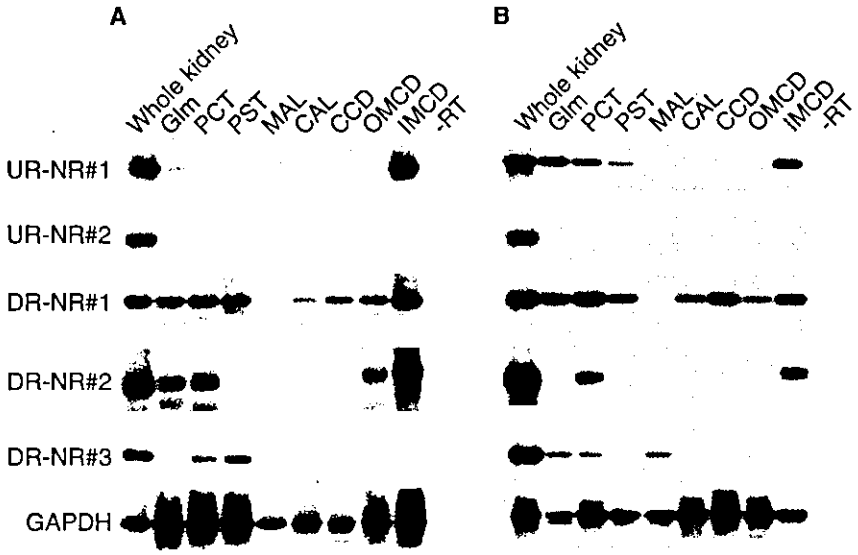

Fig. 4. Detection of mRNA of the five unknown genes in nephron segments in sham (*A*) and 5/6 nephrectomized (NR) kidney (*B*) 2 weeks after the operation by reverse transcription-polymerase chain reaction (RT-PCR) and subsequent Southern blotting. Each PCR amplification (35 cycles) was performed using a part of the reverse transcription reaction derived from 20 glomeruli or 8 mm length of renal tubule. The cDNA synthesized was amplified using sets of primers specific for each clone. The PCR products were separated by electrophoresis through 1.0% agarose gels. The agarose gels were transferred onto a nylon membrane and hybridized with the [^{32}P] deoxycytidimine triphosphate (dCTP)-labeled each cDNA as probes at high stringency. Abbreviations are: Glm, glomerulus; PCT, proximal convoluted tubule; PST, proximal straight tubule; MAL, medullary thick ascending limb; CAL, cortical thick ascending limb; CCD, cortical collecting duct; OMCD, outer medullary collecting duct; IMCD, inner medullary collecting duct; −RT, whole kidney without reverse transcriptase; UR-NR #1, up-regulated 5/6 nephrectomized #1; UR-NR #2, up-regulated 5/6 nephrectomized #2; DR-NR #1, down-regulated 5/6 nephrectomized #1; DR-NR #2, down-regulated 5/6 nephrectomized #2; DR-NR #3, down-regulated 5/6 nephrectomized #3; GADPH, glyceraldehyde-3-phosphate dehydrogenase.

Table 6. State of renal function of rats treated with cisplatin or vancomycin

	Body weight *g*	Plasma creatinine *mg/dL*	Blood urea nitrogen *mg/dL*	Creatinine clearance *mL/min/kg*	Urinary excretion of albumin *mg/day*	Urinary excretion of NAG *U/day*	Kidney weight *g*
Vehicle	333 ± 8	0.7 ± 0.0	13 ± 2	3.2 ± 0.1	0.8 ± 0.3	277 ± 32	2.2 ± 0.1
Cisplatin	268 ± 5[a]	2.7 ± 0.3[a]	105 ± 15[a]	0.5 ± 0.1[a]	3.5 ± 0.8[a]	1093 ± 241[a]	2.2 ± 0.1
Vancomycin	320 ± 11	0.8 ± 0.1	28 ± 4[a]	3.3 ± 0.4	1.9 ± 0.8	582 ± 41[a]	2.9 ± 0.2[a]

NAG is *N*-acetyl-β-D-glucosaminidase.

Rats were treated with cisplatin (6 mg/kg) intraperitonealy, vancomycin (500 mg/kg) intravenously or vehicle (saline) intravenously. Urine and blood samples were collected 3 days after the treatments. Data represent the mean ± SEM of five rats.

[a] $P < 0.05$, significantly different from vehicle (Fisher's *t* test).

DISCUSSION

Large-scale cDNA expression profiling was performed to construct the expression profiles of 5/6 nephrectomized and sham-operated kidney. In the 5/6 nephrectomized kidney, the expression of growth factor-related mRNA such as for IGF, IGFBPs, and TGF-β, which are known to directly up-regulate cell growth was increased compared to that in the sham-operated kidney (Table 1) [3, 6, 33, 34]. It is known that compensatory hypertrophy occurs at 2 weeks after nephrectomy [2]. The increase in the expression of growth factor–related genes might correspond to the compensatory hypertrophy. The mRNA-encoded cytoskeletal or membrane proteins were also increased in the 5/6 nephrectomized kidney compared to the sham-operated kidney. The increases of these mRNAs were thought to be due to the process of tissue repair and hypertrophy. In contrast to the above genes, the mRNA expression frequency related to transporters and cofactors of transporters such as OCTN2 and 4F2hc, was decreased in the 5/6 nephrectomized kidney (Table 1). Our previous reports demonstrated that the mRNA of the organic anion and the cation transporters, OAT-K and OCT2, was down-regulated, accompanied by a decrease in the urinary excretion of methotrexate and cimetidine, respectively, in the 5/6 nephrectomized rats [9, 10]. The decrease in transporter-related genes shown in this study might account for the reduction of urinary excretion of various drugs in CRF. Taken together, these changes observed in the 5/6 nephrectomized and in the sham-operated kidney databases could account for the physiologic state of the residual kidneys in 5/6 nephrectomized rats.

To confirm whether the in silico subtractive database of 5/6 nephrectomized kidney reflected the actual expression of mRNA or protein, the expression of 12 genes, which have been considered to play significant roles in the kidney, was examined by Northern blotting or Western blotting in the 5/6 nephrectomized and in the sham-operated kidney (Table 4). The differential expression

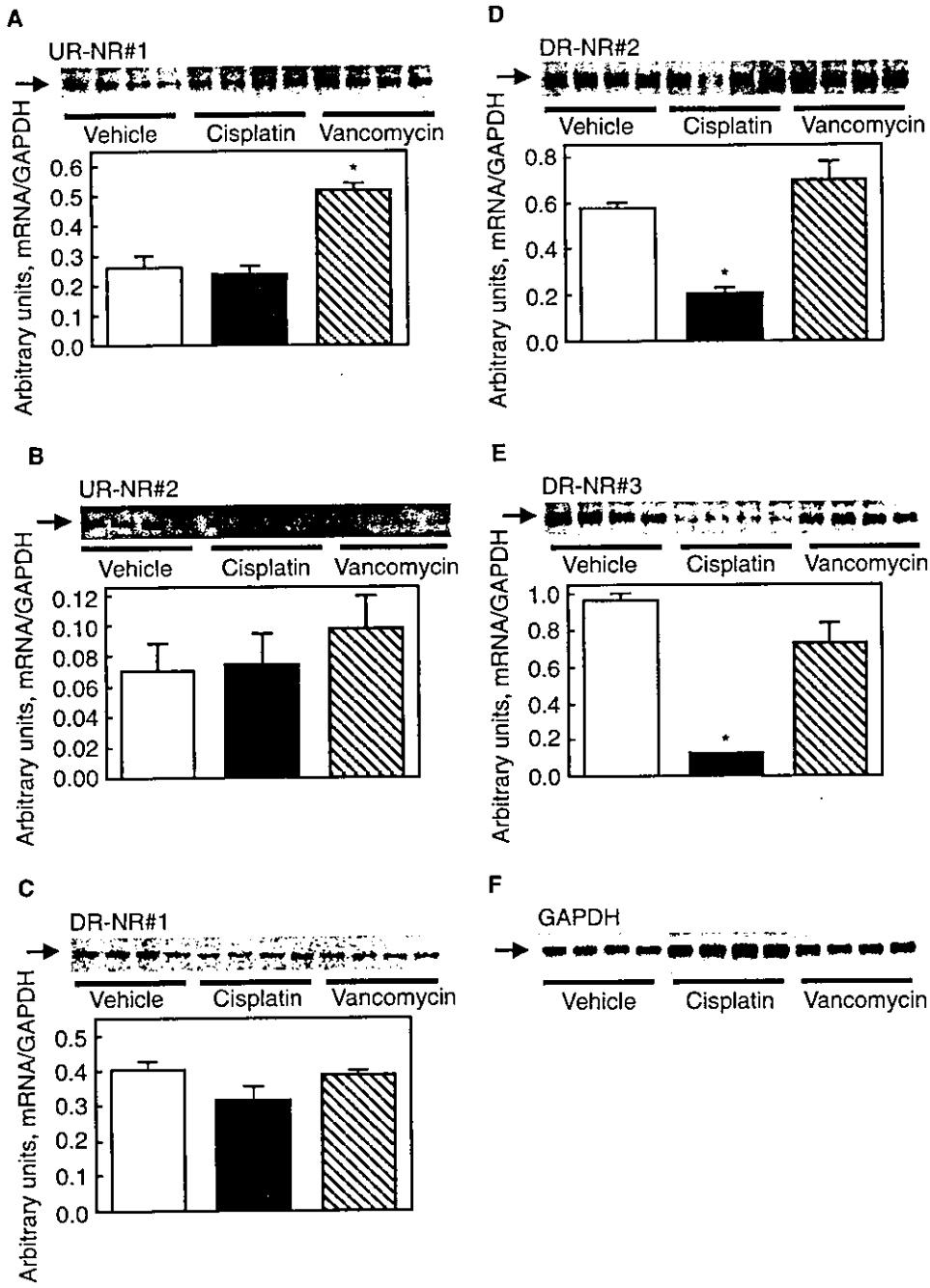

Fig. 5. Northern blotting of the five unknown genes in the rats treated with cisplatin or vancomycin. Expression of up-regulated 5/6 nephrectomized (UR-NR) #1 mRNA (*A*), up-regulated 5/6 nephrectomized (UR-NR) #2 mRNA (*B*), down-regulated 5/6 nephrectomized (DR-NR) #1 mRNA (*C*), down-regulated 5/6 nephrectomized (DR-NR) #2 mRNA (*D*), down-regulated 5/6 nephrectomized (DR-NR) #3 (*E*), and glyceraldehyde-3-phosphate dehydrogenase (GAPDH) mRNA (*F*) in vehicle, cisplatin, or vancomycin-treated rat kidneys was examined. Five micrograms of total RNA of kidneys was hybridized with each probe under high stringency conditions. The amounts of mRNA were quantified by densitometry and normalized to GAPDH. Each column represents the mean ± SEM of four rats. $^*P < 0.05$, significantly different from vehicle-treated rats (Fisher's *t* test).

patterns of these 12 genes between the 5/6 nephrectomized and sham-operated kidney databases were comparable with the results of Northern blotting and Western blotting (Fig. 1). Thus, the results indicated that the frequency shown in this subtractive database was reliable enough to estimate actual expression of mRNA and protein.

Digital expression profiling has been used to analyze gene expression on a large scale [15–18]. With this technique, cDNA was digested by the restriction enzyme

Table 7. The orthologues of the five unknown putative proteins

Clone ID	Accession number	Gene name of orthologues	Homology	Accession number of orthologues	
				Nucleotide	Protein
UR-NR #1	AB108667	Mus musculus 10 days embryo putative protein	97%	AK012030	BAB27984
UR-NR #2	AB108668	Mus musculus clone MGC:11983	97%	BC011420	AAH11420
DR-NR #1	AB108669	Mus musculus NN5H6H tumor-related protein mRNA	99%	AY035213	AAK64607
DR-NR #2	AB108670	Homo sapiens hypothetical protein DKFZp564B1162	82%	NM_031305	NP_112595
DR-NR #3	AB108671	Homo sapiens CGI-86 protein	61%	XM_055115	XP_055115

The ortholog of the five unknown deduced amino acid proteins differentially expressed in the 5/6 nephrectomized kidney are listed. Homology was estimated by GENETYX-MAC, version 10.1.

A UR-NR#1

```
  1 MQKSCDENEGTPQNTPKADEGHPSEDPPQQAGENLQASGENVREETDGSLRGEPAEPSPE
 61 PKEDTPARHLNPEEVIRGVDELERLREEIRRVRNKFVLMHWEQRHSRSRPYPVCFRP
```

B UR-NR#2

```
  1 MVVQAKKRELKEAQRRKKQLEERCKVEESIGNAVLTWNNEILPNWETMWCSKKVRDLWWQ
 61 GIPPSVRGKVWSLAMGNEVNITHELFDICFARAKERWRSLSTGGSEVENEDAGFSAADRE
121 ASLELIKLDISRTFPNLCIFQQGGFYHDMLHSILGAYTCYRPDVGYVQGMSFIAAVLILN
181 LDTADAFIAFSNLLNKPCQMAFFRVDHGLMLTYFAAFEVFFEENLPKLFAHFKKNNLTAD
241 IYLIDWIFTLYSKSLPLDLACRIWDVFCRDGEEFLFRTALGILKLFEDILTRMDFIHSAQ
301 FLTRLPEDLPADDVFAAISTVQMQSRNKKWAQVLSALQKDSREMEEGSPSVRD
```

C DR-NR#1

```
  1 MAAAEPSVAALAGGGVGAGAPSGGVPVLFCFSVFARPASVPHGAGYDVLIQKFLSLYGDQ
 61 VDMHRKFVVQLFAEEWGQYVDLPKGFAVSERCKLRLVPLQIQLTTLGNLTPPSTVFFCCD
121 MQERFRPAIKYFGDIISVGQRLLQGARILGIPVIITEQYPKGLGSTVQEIDLTGVKLVLP
181 KTKFSMVLPEVEAALAEIPGVRSVVLFGVETHVCIQQTALELVGRGIEVHIVADATSSRS
241 MMDRMFALERLARTGIIVTTSEAVPLQLVADKDHPKFKEIQNLIKASAPESGLLSKV
```

D DR-NR#2

```
  1 MLVEQCVDFIRQRGLKEEGLFRLPGQANLVKELQDAFDCGEKPSFDSNTDVETVASLLKL
 61 YLRELPEPVVPYAKYEDFLSCATLLSKEEEAGVKELTKQVKSLPVVNYNLLKYICRFLDE
121 VQSYSGVNKMSAQNLATVFGPNILRPKVEDPLTIMEGTVVVQQLMSVMISKHDRLFPKDT
181 EPQSKPQEGPNSNNNDGHKKVTIGQLQNKENNNTKESPVRRCSWDKPESPQRSSMDNGSP
241 TALSGSKTNSPRNSIHKLDVSRSPPLTVKKNPAFNKGRGIVTNGSFSSSNGEGVEKTQTT
301 PNGSLQARRSSSLESSGTKWGTHSVQNGTVRMGYLNTDTLGNSLNGRSMSWLPNGYVTLR
361 DNKQKEPGGESSQHNRLSTYDNVHQQFSLMNLDDKHRVDSATWSTSSCEISLPENSNSCR
421 SSTTTCPEQDFYGGNFEDPVLDGPPQDDLSHPGDYENKSDRRSVGGRSSRATSSSDNSDT
481 FFGNTSSNHSALHSLVSSLKQEMTRQKIEYESRIKSLEQRNLTLETEMLNLHDELDQERK
541 KFTMIEIKMRNAERAKEDAEKRNDMLQKEMEQFFSTFGDLTVEPRRSERGNTIWIQ
```

E DR-NR#3

```
DR-NR#3    1 : MMGFEFWMLA LCALLLLVLG LLSFLWLDSD LTLLRAAWMG QCPEQALADK VVWIYGASSG

DR-NR#3   61 : IGEELAFQLS KLGVCLVLSA RRGQELEHVK RRCLENGNLK EKDILVLPLD LADTSSHDIA
Rat S-2    1 :                             VK RRSLENGNLK EKDILVLPLD LADTSSHDIA

DR-NR#3  121 : TKTVLQEFGR IDILVNNGGV AHASLVENTN MDIFKVLIEV NYLGTVSLTK CVLPHMMERN
Rat S-2   33 : TKTVLQEFGR IDILVNNGGV AHASLVENTN MDIFKVLIEV NYLGTVSLTK CFLPHMMERN

DR-NR#3  181 : QGKIVVMKSL VGIVPRPLCS GYAASKLALR GFFDVLRTEL FDYPGITLSM ICPGPVHSNI
Rat S-2   93 : QGKIVVMKS 101

DR-NR#3  241 : FQNAFTGDFT ETRLPKIPLF KMETSRCVQL ILVSLANDLE DIWIANQPVL LRAYVWQYVP

DR-NR#3  301 : FRDWILQGRY GKYISKVLGI TWYR
```

Fig. 6. The deduced amino acid sequences of the five unknown genes. (*A*) Up-regulated 5/6 nephrectomized (UR-NR) #1 encoded a putative protein of 117 amino acids that are shown in the one-letter code. (*B*) Up-regulated 5/6 nephrectomized (UR-NR) #2 encoded a putative protein of 353 amino acids that are shown in the one-letter code. The region in bold is highly homologous with the TBC domain. (*C*) Down-regulated 5/6 nephrectomized (DR-NR) #1 encoded a putative protein of 298 amino acids that are shown in the one-letter code. The region in bold is highly homologous with the conserved domain of isocholismatase. (*D*) Down-regulated 5/6 nephrectomized (DR-NR) #2 encoded a putative protein of 596 amino acids that are shown in the one-letter code. The region in bold is highly homologous with the conserved domain of Rho-GAPs. (*E*) Down-regulated 5/6 nephrectomized (DR-NR) #3 encoded a putative protein of 324 amino acids that are shown in the one-letter code. The sequences of TGxxxGxG (boxed with a thick line and in bold) indicate the NADPH binding site. The sequences of S-Y-K (bold region) indicate the short chain dehydrogenase active site motif. An alignment with rat S-2 protein is also presented. Conserved residues between two proteins are boxed.

Table 8. The conserved domains of the five unknown deduced amino acid proteins

Clone ID	Region	Definition	E value	Accession number
UR-NR #1[a]	—	—	—	—
UR-NR #2	58–294	TBC domain	6.0E-42	pfam00566
DR-NR #1	109–265	Isochorismatase family	1.3E-07	pfam00857
DR-NR #2	1–173	RhoGAP domain	2.0E-44	pfam00620
DR-NR #3	48–294	Short chain dehydrogenase	2.3E-46	pfam00106

Motifs of the five unknown putative proteins were searched against the Smart and Pfam libraries.

[a]There was no conserved domain in UR-NR #1.

*Mbo*I and sequenced from the 3′ end. However, in our study, cDNA libraries were constructed without cleaving using *Mbo*I, and the cDNA inserts were sequenced from the 5′ end. In many cases the sequenced region from the 5′ end is different in the same genes, because full-length cDNAs are not always isolated. However, the identity of two genes in which sequenced regions are different can be easily examined by homology search, because the number of enrolled genes in Genbank, EMBL, or DDBJ has markedly increased recently. In this study, the genes not identified by BLAST search were further sequenced from the 3′ end to determine their identity. So, the sequence from the 5′ end used in this study should be suitable for digital expression profiling. In a previous digital expression profiling, about 70% of mouse renal proximal tubule genes and renal collecting duct genes were novel genes unidentified by homology search [17, 18]. In contrast, only 17% of 2048 sequenced genes were novel in the present study (Table 1). It was reported that the noncoding regions of the 3′ end are sometimes variant among species or tissues [35, 36]. This might be one of the reasons why there were so many novel genes not identified by BLAST search in previous studies. Consequently, the sequence from the 5′ end appeared to be more useful for digital expression profiling.

Although a previous report mentioned that cleaving cDNA by *Mbo*I could normalize the cloning efficiencies reflecting the size or base composition of cDNA [15], we constructed cDNA libraries without cleaving to sequence from the 5′ end. Nevertheless, this subtractive database of 5/6 nephrectomized kidney well reflected the actual expression of mRNA or protein as mentioned above. In addition, GAPDH mRNA, which is abundantly and ubiquitously expressed and often used as an internal control, appeared both in the 5/6 nephrectomized and sham-operated kidney databases four and six times, respectively (Table 4). However, abundantly appearing GAPDH was not observed in other digital expression profiles [15, 17, 18]. Although the reason for the difference between this study and the other studies remains unknown, the results of the present study are thought to more reasonably reflect the actual mRNA expression.

A subtractive analysis of 5/6 nephrectomized mouse kidney using the cDNA-RDA technique has been reported by Zhang et al [19]. Several genes up-regulated in the 5/6 nephrectomized mouse kidney were successfully isolated, but genes previously known to increase after 5/6 nephrectomy were not isolated in their study. In contrast, in our study, KIM-1 and osteopontin mRNA, which were reported to increase upon renal injury [37–39], also increased in the 5/6 nephrectomized kidney database (Table 2). This subtractive database reflected previous reports on the 5/6 nephrectomized rat, and might be useful to search for the molecular mechanisms of CRF.

We successfully isolated five unknown genes expressed differently between in the 5/6 nephrectomized and sham-operated kidney by in silico subtraction (Fig. 2). The ratio of false positive clones that failed to show their up- or down-regulated expression was 70% (13 clones out of 18), which was much lower than that of the previous reports (over 80%) in which differential display was used [19, 40, 41]. Although all five are highly homologous to known human or mouse genes, little information is available concerning the functions and tissue distributions of these hypothetical genes. Their expression patterns in the earlier phase of 5/6 nephrectomized kidney and other renal failure models might be useful to speculate their roles in such conditions as hypertrophy of kidneys, tissue repair, blood pressure, and albuminuria. The precise physiologic roles of these five genes could not be discussed only from these expression data and the structure. However, it could be speculated that DR-NR #3 might serve as a biomarker for renal tubular injury by CRF, such as KIM-1, which is a transmembrane protein of proximal tubule and is thought to serve as a urinary marker for acute renal tubular injury [42]. In addition, UR-NR #2 and DR-NR #1 might be involved in the pathology induced by the reduction of renal mass, because the mRNA expression level of these two genes was maintained in the kidneys impaired by cisplatin or vancomycin (Fig. 5B and C). Particularly, UR-NR #2 might be involved in the compensatory hypertrophy, as it was sequentially increased in 5/6 nephrectomized kidneys in parallel to the kidney weights. Further physiologic or pathophysiologic studies, including the individual variations of expression levels, are needed to elucidate the roles of these five unknown genes in the progressive nephropathy.

Digital databases based on random sequencing reflect the mRNA expression profiles for relatively highly expressed genes [17, 18, 20]. Although we performed in silico subtraction only between 5/6 nephrectomized and sham-operated kidney databases, this methodology enables us to create disease-specific gene subsets using various disease models, as well as body mapping [15, 16].

CONCLUSION

We constructed subtractive expression databases of 5/6 nephrectomized and sham-operated kidney, which reflected the actual alterations of mRNA expression caused by subtotal nephrectomy, and was suggested to be useful for analysis of the molecular mechanisms of CRF. In addition, we successfully isolated five unknown genes expressed differently in the 5/6 nephrectomized kidney from in silico subtraction, two of which were up-regulated and three down-regulated. Although these five genes might be involved in the progression and/or restoration of CRF, further studies are needed to elucidate their roles in the pathogenesis of CRF.

ACKNOWLEDGMENTS

This work was supported by a Grant-in-Aid for Research on Human Genome, Tissue Engineering, and Food Biotechnology H12-Genome-019 from the Ministry of Health, Labor, and Welfare of Japan, by a Grant-in-Aid for Scientific Research from the Ministry of Education, Culture, Sports, Science, and Technology of Japan, and by the 21st Century COE Program "Knowledge Information Infrastructure for Genome Science." The nucleotide sequences reported in this article have been submitted to the GenBank with accession numbers between AB108667 and AB108671.

Reprint requests to Professor Ken-ichi Inui, Ph.D., Department of Pharmacy, Kyoto University Hospital, Sakyo-ku, Kyoto 606–8507, Japan.
E-mail: inui@kuhp.kyoto-u.ac.jp

REFERENCES

1. Hostetter TH, Olson JL, Rennke HG, *et al*: Hyperfiltration in remnant nephrons: A potentially adverse response to renal ablation. *J Am Soc Nephrol* 12:1315–1325, 2001
2. Waldherr R, Gretz N: Natural course of the development of histological lesions after 5/6 nephrectomy. *Contrib Nephrol* 60:64–72, 1988
3. Ali SM, Laping NJ, Fredrickson TA, *et al*: Angiotensin-converting enzyme inhibition attenuates proteinuria and renal TGF-beta 1 mRNA expression in rats with chronic renal disease. *Pharmacology* 57:20–27, 1998
4. Floege J, Alpers CE, Burns MW, *et al*: Glomerular cells, extracellular matrix accumulation, and the development of glomerulosclerosis in the remnant kidney model. *Lab Invest* 66:485–497, 1992
5. Grønboek H, Nielsen B, Flyvbjerg A, Ørskov H: Effect of graded renal ablation on kidney and serum insulin-like growth factor-I (IGF-I) and IGF binding proteins in rats: Relation to compensatory renal growth. *Metabolism* 46:29–35, 1997
6. Muchaneta-Kubara EC, Sayed-Ahmed N, el Nahas AM: Subtotal nephrectomy: A mosaic of growth factors. *Nephrol Dial Transplant* 10:320–327, 1995
7. Totsune K, Mackenzie HS, Totsune H, *et al*: Upregulation of atrial natriuretic peptide gene expression in remnant kidney of rats with reduced renal mass. *J Am Soc Nephrol* 9:1613–1619, 1998
8. Benigni A, Zoja C, Corna D, *et al*: Blocking both type A and B endothelin receptors in the kidney attenuates renal injury and prolongs survival in rats with remnant kidney. *Am J Kidney Dis* 27:416–423, 1996
9. Ji L, Masuda S, Saito H, Inui K: Down-regulation of organic cation transporter rOCT2 by 5/6 nephrectomy. *Kidney Int* 62:514–524, 2002
10. Takeuchi A, Masuda S, Saito H, *et al*: Role of kidney-specific organic anion transporters in the urinary excretion of methotrexate. *Kidney Int* 60:1058–1068, 2001
11. Hubank M, Schatz DG: Identifying differences in mRNA expression by representational difference analysis of cDNA. *Nucleic Acids Res* 22:5640–5648, 1994
12. Liang P, Pardee AB: Differential display of eukaryotic messenger RNA by means of the polymerase chain reaction. *Science* 257:967–971, 1992
13. Bowtell DD: Options available—from start to finish—for obtaining expression data by microarray. *Nat Genet* 21(Suppl):25–32, 1999
14. Gerhold D, Rushmore T, Caskey CT: DNA chips: Promising toys have become powerful tools. *Trends Biochem Sci* 24:168–173, 1999
15. Okubo K, Hori N, Matoba R, *et al*: A novel system for large-scale sequencing of cDNA by PCR amplification. *DNA Seq* 2:137–144, 1991
16. Okubo K, Hori N, Matoba R, *et al*: Large scale cDNA sequencing for analysis of quantitative and qualitative aspects of gene expression. *Nat Genet* 2:173–179, 1992
17. Takenaka M, Imai E, Kaneko T, *et al*: Isolation of genes identified in mouse renal proximal tubule by comparing different gene expression profiles. *Kidney Int* 53:562–572, 1998
18. Takenaka M, Imai E, Nagasawa Y, *et al*: Gene expression profiles of the collecting duct in the mouse renal inner medulla. *Kidney Int* 57:19–24, 2000
19. Zhang H, Wada J, Kanwar YS, *et al*: Screening for genes upregulated in 5/6 nephrectomized mouse kidney. *Kidney Int* 56:549–558, 1999
20. Horiba N, Masuda S, Takeuchi A, *et al*: Cloning and characterization of a novel Na^+-dependent glucose transporter (NaGLT1) in rat kidney. *J Biol Chem* 278:14669–14676, 2003
21. Horiba N, Masuda S, Ohnishi C, *et al*: Na^+-dependent fructose transport via rNaGLT1 in rat kidney. *FEBS Lett* 546:276–280, 2003
22. Matsumura Y, Uchida S, Kondo Y, *et al*: Overt nephrogenic diabetes insipidus in mice lacking the CLC-K1 chloride channel. *Nat Genet* 21:95–98, 1999
23. Nakamura T, Kokuryo T, Hashimoto Y, Inui K: Effects of fosfomycin and imipenem-cilastatin on the nephrotoxicity of vancomycin and cisplatin in rats. *J Pharm Pharmcol* 51:227–232, 1999
24. Saito H, Masuda S, Inui K: Cloning and characterization of a novel rat organic anion transporter mediating basolateral uptake of methotrexate. *J Biol Chem* 271:20719–20725, 1996
25. Ogihara H, Saito H, Shin BC, *et al*: Immuno-localization of H^+/peptide cotransporter in rat digestive tract. *Biochem Biophy Res Commun* 220:848–852, 1996
26. Masuda S, Saito H, Nonoguchi H, *et al*: mRNA distribution and membrane localization of the OAT-K1 organic anion transporter in rat renal tubules. *FEBS Lett* 407:127–131, 1997
27. Vollmer P, Will E, Scheglmann D, *et al*: Primary structure and biochemical characterization of yeast GTPase-activating proteins with substrate preference for the transport GTPase Ypt7p. *Eur J Biochem* 260:284–290, 1999
28. Romao MJ, Turk D, Gomis-Ruth FX, *et al*: Crystal structure analysis, refinement and enzymatic reaction mechanism of *N*-carbamoylsarcosine amidohydrolase from *Arthrobacter sp.* at 2.0 Å resolution. *J Mol Biol* 226:1111–1130, 1992
29. Li R, Zhang B, Zheng Y: Structural determinants required for the interaction between Rho GTPase and the GTPase-activating domain of p190. *J Biol Chem* 272:32830–32835, 1997
30. Ridley AJ: The GTP-binding protein Rho. *Int J Biochem Cell Biol* 29:1225–1229, 1997
31. Terada T, Sugihara Y, Nakamura K, *et al*: Cloning and bacterial expression of monomeric short-chain dehydrogenase/reductase (carbonyl reductase) from CHO-K1 cells. *Eur J Biochem* 267:6849–6857, 2000
32. Iwai N, Inagami T: Isolation of preferentially expressed genes in the kidneys of hypertensive rats. *Hypertension* 17:161–169, 1991
33. Svegliati-Baroni G, Ridolfi F, Di Sario A, *et al*: Insulin and insulin-like growth factor-1 stimulate proliferation and type I collagen accumulation by human hepatic stellate cells: Differential effects on signal transduction pathways. *Hepatology* 29:1743–1751, 1999
34. Han DC, Isono M, Hoffman BB, Ziyadeh FN: High glucose stimulates proliferation and collagen type I synthesis in renal cortical fibroblasts: Mediation by autocrine activation of TGF-beta. *J Am Soc Nephrol* 10:1891–1899, 1999

35. LaForge KS, Unterwald EM, Kreek MJ: Structure and expression of the guinea pig preproenkephalin gene: Site-specific cleavage in the 3′ untranslated region yields truncated mRNA transcripts in specific brain regions. *Mol Cell Biol* 15:2080–2089, 1995
36. Ferrari S, Battini R, Kaczmarek L, *et al*: Coding sequence and growth regulation of the human vimentin gene. *Mol Cell Biol* 6: 3614–3620, 1986
37. Yu XQ, Wu LL, Huang XR, *et al*: Osteopontin expression in progressive renal injury in remnant kidney: Role of angiotensin II. *Kidney Int* 58:1469–1480, 2000
38. Persy VP, Verstrepen WA, Ysebaert DK, *et al*: Differences in osteopontin up-regulation between proximal and distal tubules after renal ischemia/reperfusion. *Kidney Int* 56:601–611, 1999
39. Ichimura T, Bonventre JV, Bailly V, *et al*: Kidney injury molecule-1 (KIM-1), a putative epithelial cell adhesion molecule containing a novel immunoglobulin domain, is up-regulated in renal cells after injury. *J Biol Chem* 273:4135–4142, 1998
40. Gaede KI, Mamat U, Schlaak M, Muller-Quernheim J: Analysis of differentially regulated mRNAs in monocytic cells induced by in vitro stimulation. *J Mol Med* 77:847–852, 1999
41. Roschier M, Kuusisto E, Salminen A: A differential display protocol to identify differentially expressed mRNAs in potassium-deprived cerebellar granule cells. *Brain Res Protoc* 5:121–131, 2000
42. Han WK, Bailly V, Abichandani R, *et al*: Kidney injury molecule-1 (KIM-1): A novel biomarker for human renal proximal tubule injury. *Kidney Int* 62:237–244, 2002

Available online at www.sciencedirect.com

SCIENCE DIRECT

European Journal of Pharmacology 503 (2004) 25–30

ELSEVIER

ejp

www.elsevier.com/locate/ejphar

Different transport properties between famotidine and cimetidine by human renal organic ion transporters (SLC22A)

Hideyuki Motohashi, Yuichi Uwai, Kiyo Hiramoto, Masahiro Okuda, Ken-ichi Inui*

Department of Pharmacy, Kyoto University Hospital, Faculty of Medicine, Kyoto University, Sakyo-ku, Kyoto 606-8507, Japan

Received 3 May 2004; received in revised form 2 September 2004; accepted 14 September 2004
Available online 12 October 2004

Abstract

Histamine H_2 receptor antagonist famotidine and cimetidine are commonly used for treatment of gastrointestinal ulcer diseases. Inasmuch as these drugs are mainly secreted by renal tubules, dosages have been adjusted according to renal function. Although many studies have been performed on the molecular mechanisms of renal handling of cimetidine, little is known about that of famotidine. In this study, to examine the recognition and transport of famotidine by human organic anion transporters (OATs; hOAT1, hOAT3) and human organic cation transporter (OCT; hOCT2), the uptake studies using *Xenopus laevis* oocytes were performed in comparison with cimetidine. The half-maximal inhibitory concentrations of famotidine for [^{3}H]estrone sulfate transport by hOAT3 and [^{14}C]tetraethylammonium transport by hOCT2 (300 μM and 1.8 mM, respectively) were higher than those of cimetidine (53 and 67 μM, respectively). While cimetidine inhibited *p*-[^{14}C]aminohippurate transport by hOAT1 in a concentration dependent manner, famotidine did not affect it at 5 mM. In addition, hOAT3 mediated famotidine uptake, but hOAT1 and hOCT2 did not show famotidine transport. These results indicate that there are marked differences between famotidine and cimetidine in the recognition and transport by organic ion transporters and that hOAT3 contributes to the renal tubular secretion of famotidine. Present findings should be useful information to understand the renal handling of famotidine and cimetidine.
© 2004 Elsevier B.V. All rights reserved.

Keywords: Organic anion transporter; Organic cation transporter; Famotidine; Cimetidine; Renal tubular secretion

1. Introduction

A histamine H_2 receptor antagonist famotidine is commonly used in the treatment for gastrointestinal ulcer diseases. Famotidine shows beneficial characteristics, including stronger inhibition of gastric acid secretion, longer acting and less interaction with P-450, compared with another histamine H_2 receptor antagonist cimetidine (Howard et al., 1985; Humphries, 1987). Pharmacokinetic studies revealed that famotidine was mainly excreted into the urine as an unmetabolized form (Takabatake et al., 1985; Lin et al., 1988; Dowling et al., 2001). Renal clearance of famotidine exceeded the creatinine clearance about three times in subjects with normal renal function, indicating the efficient tubular secretion of the drug. In patients with renal insufficiency, plasma elimination and renal clearance of famotidine were significantly decreased (Takabatake et al., 1985; Lin et al., 1988). To avoid the accumulation and undesirable effects, famotidine dosage should be reduced according to the renal functions.

In this decade, organic anion transporters (OATs) and organic cation transporters (OCTs) in the kidney were identified, and their characteristics have been clarified. These transporters mediate endogenous and exogenous substances, such as uremic toxins, diuretics, methotrexate, antibiotics, antivirals and nonsteroidal antiinflammatory drugs, suggesting that OATs and OCTs are responsible for the tubular secretion of these compounds (Inui et al., 2000; Sekine et al., 2000; Dresser et al., 2001). Recently, we quantified mRNA levels of organic ion transporters in the

* Corresponding author. Tel.: +81 75 751 3577; fax: +81 75 751 4207.
E-mail address: inui@kuhp.kyoto-u.ac.jp (K. Inui).

0014-2999/$ - see front matter © 2004 Elsevier B.V. All rights reserved.
doi:10.1016/j.ejphar.2004.09.032

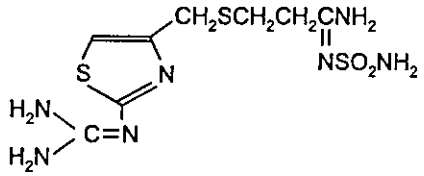

Famotidine

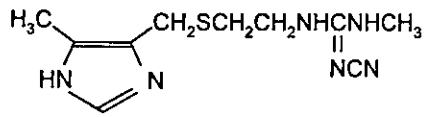

Cimetidine

Fig. 1. Chemical structures of famotidine and cimetidine.

human kidney cortex and revealed that hOAT1 (SLC22A6), hOAT3 (SLC22A8) and hOCT2 (SLC22A2) mRNA were higher than other organic ion transporters (Motohashi et al., 2002). Moreover, hOAT1, hOAT3 and hOCT2 protein localized at the basolateral membrane of the renal proximal tubules. Accordingly, these transporters play important roles for the renal uptake of organic compounds from the circulation.

It has been assumed that the renal tubular secretion of famotidine and cimetidine would be mediated by OCTs due to their cationic property at the physiological pH (Fig. 1). Indeed, cimetidine inhibits the renal secretion of various organic cations (Somogyi et al., 1983; Christian et al., 1984; van Crugten et al., 1986) and Urakami et al. (2001, 2002) indicated that rat and human organic cation transporters rOCT1, rOCT2 and hOCT2 transported cimetidine. However, in addition to hOCT2, hOAT1, hOAT3 and rOAT3 were shown to transport the cimetidine. (Kusuhara et al., 1999; Cha et al., 2001; Burckhardt et al., 2003). Therefore, it was supposed that these three transporters were concerned with renal secretion of cimetidine. While famotidine is more frequently used than cimetidine because of it beneficial characteristics, adverse effects associated with famotidine, such as thrombocytopenia (Wade et al., 2002) or central nerve system reaction (Yoshimoto et al., 1994), have been reported. Although dosage should be adjusted according to renal function, molecular mechanisms of renal secretion of famotidine have not been investigated in contrast to cimetidine. To understand the renal handling of famotidine, it should be examined whether hOATs or hOCTs recognize and transport famotidine.

The purpose of the present study is to clarify the recognition and transport properties of famotidine by hOAT1, hOAT3 and hOCT2 in comparison with cimetidine. We performed transport experiments of famotidine and cimetidine using *Xenopus laevis* oocytes expressing these organic ion transporters.

2. Materials and methods

2.1. Materials

p-[Glycyl-^{14}C]aminohippurate (PAH; 1.9 GBq/mmol), [1-^{14}C]tetraethylammonium bromide (TEA; 88.8 MBq/mmol) and [6,7-^{3}H(N)]estrone sulfate were obtained from Perkin-Elmer Life Science Products (Boston, MA, USA). Famotidine and cimetidine were purchased from Wako Pure Chemical Industries (Osaka, Japan) and Nacalai Tesque (Kyoto, Japan), respectively. Unlabeled PAH and estrone 3-sulfate were from Sigma (St. Louis, MO, USA). 1-Methyl-4-phenylpyridinium (MPP) was from Research Biochemicals International (Natick, MA, USA). All other chemicals used were of the highest purity available.

2.2. Transport experiments using X. laevis oocytes expressing hOAT1, hOAT3 and hOCT2

Functional analyses of the organic ion transporters using *X. laevis* oocytes were carried out according to our previous report (Uwai et al., 2000). Briefly, the capped cRNA was transcribed from *Xba*I-linearized pSPORT1 containing hOAT1, hOAT3 or hOCT2 cDNA with T7 RNA polymerase. After the injection of 50 nl of water or the cRNA (25 ng) into oocytes, the oocytes were maintained in modified Barth's medium (88 mM NaCl, 1 mM KCl, 0.33 mM

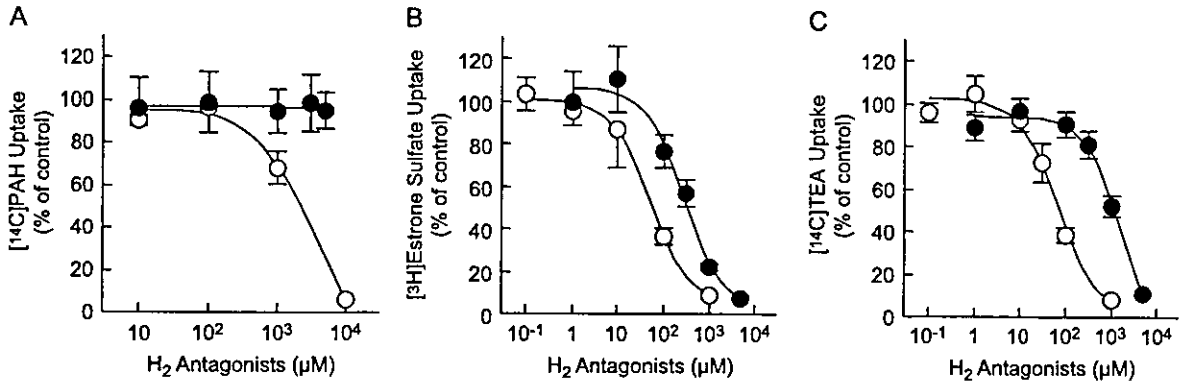

Fig. 2. Inhibitory effects of famotidine and cimetidine on organic ion uptake by hOAT1 (A)-, hOAT3 (B)- and hOCT2 (C)-expressing oocytes. hOAT1-, hOAT3- or hOCT2-expressing oocytes were incubated with 25 μM [^{14}C]PAH, 18.87 nM [^{3}H]estrone sulfate or 36 μM [^{14}C]TEA, respectively, in the absence (control) or presence of famotidine (●) or cimetidine (○) at various concentrations for 1 h. Each point represents the mean±S.E.M. of 7 to 10 oocytes.

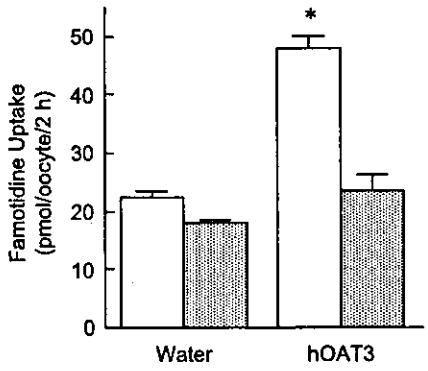

Fig. 3. Uptake of famotidine by hOAT3-expressing oocytes. Water-injected or hOAT3-expressing oocytes were incubated with 1 mM famotidine in the absence (open column) or presence (dotted column) of 1 mM estrone sulfate for 2 h. Each column represents the mean±S.E.M. of five to eight measurements. Four oocytes were used for each uptake measurement. *$P<0.05$, significantly different from the other three columns.

$Ca(NO_3)_2$, 0.4 mM $CaCl_2$, 0.8 mM $MgSO_4$, 2.4 mM $NaHCO_3$ and 10 mM HEPES; pH7.4) with 50 μg/ml of gentamicin at 18 °C for 3 days. The uptake reaction of [^{14}C]PAH, [^{3}H]estrone sulfate or [^{14}C]TEA was initiated in a 24-well plate by incubating the oocytes in 500 μl of uptake buffer (96 mM NaCl, 2 mM KCl, 1.8 mM $CaCl_2$, 1 mM $MgCl_2$ and 5 mM HEPES; pH7.4) in the absence or presence of each histamine H_2 receptor antagonist for 1 h at 25 °C. After washing the oocytes with 2 ml of ice-cold uptake buffer five times, each oocyte was transferred to a scintillation vial and dissolved in 300 μl of 10% sodium lauryl sulfate. The inhibitory effects of famotidine and cimetidine were evaluated by measuring the radioactivity of each solubilized oocyte in 3 ml of Aqueous Counting Scintillant (ACS) II (Amersham International, Buckinghamshire, UK). Uptake experiments of famotidine and cimetidine were performed by incubating oocytes in 100 μl of the uptake buffer with or without each transporter's specific inhibitor for 2 h at 25 °C in a 1.5-ml tube. After the incubation, the oocytes were washed with 1.5 ml of ice-cold uptake buffer three times. Two hundred microliters of extraction solution (30 mM phosphate buffer [pH7.0] in methanol at 1:1) was added into the tubes and sonicated. The homogenate was centrifuged at 14,000 rpm for 20 min, and the supernatant was filtrated through a Millipore filter (SJGVL; 0.45 μM). Famotidine and cimetidine taken up by oocytes were determined by high-performance liquid chromatography.

2.3. Quantification of famotidine and cimetidine by high-performance liquid chromatography

High-performance liquid chromatograph LC-10AS (Shimadzu, Kyoto, Japan) equipped with a UV spectrophotometric detector (SPD-10AV; Shimadzu) and an integrator (Chromatopac C-R1A; Shimadzu) was used for the measurement of famotidine and cimetidine under the following conditions: column, TSK-gel ODS 80TM with 4.6-mm inside diameter and 150-mm length (Tosoh, Tokyo, Japan); mobile phase, 30 mM phosphate buffer (pH7.0) in methanol at 82:18 for famotidine and 70:30 for cimetidine; flow rate, 0.8 ml/min; wavelength, 266 nm for famotidine and 235 nm for cimetidine; and temperature, 40 °C. The detection limit was 0.2 μM for famotidine and 0.1 μM for cimetidine.

2.4. Statistical analysis

Statistical analysis was performed by the one-way analysis of variance followed by Scheffe's test.

3. Results

3.1. Inhibitory effects of famotidine and cimetidine on hOAT1, hOAT3 and hOCT2

To assess whether famotidine interacts with hOAT1, hOAT3 and hOCT2, we examined its inhibitory effects on organic ion transporters (Fig. 2). Famotidine at 5 mM completely inhibited [^{3}H]estrone sulfate transport by hOAT3 and [^{14}C]TEA transport by hOCT2 but did not affect [^{14}C]PAH uptake by hOAT1. To compare the inhibitory potencies of famotidine for the transport activity

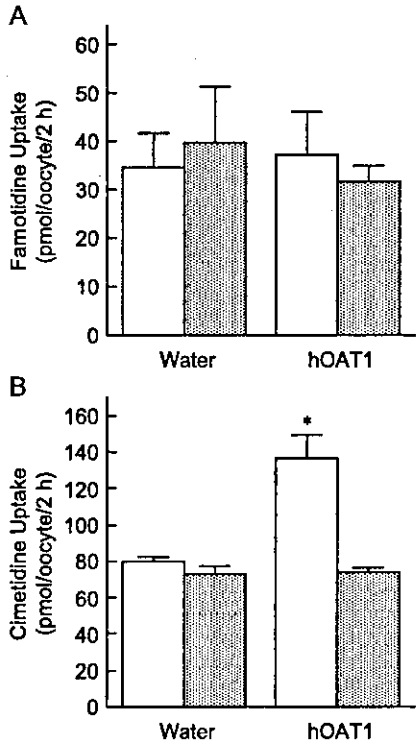

Fig. 4. Uptake of famotidine (A) and cimetidine (B) by hOAT1-expressing oocytes. Water-injected or hOAT1-expressing oocytes were incubated with famotidine or cimetidine at 2 mM in the absence (open column) or presence (dotted column) of 1 mM PAH for 2 h. Each column represents the mean±S.E.M. of five to eight measurements. Four oocytes were used for each uptake measurement. *$P<0.05$, significantly different from the other three columns.

of hOAT3 and hOCT2 with those of cimetidine, half-maximal inhibitory concentrations (IC_{50}) were estimated. As shown in Fig. 2B and C, the apparent IC_{50} values of famotidine were estimated to be 300 μM for hOAT3 and 1.8 mM for hOCT2. On the other hand, the apparent IC_{50} values of cimetidine were 53 and 67 μM for hOAT3 and hOCT2, respectively (Fig. 2B and C). In contrast to famotidine, cimetidine inhibited the transport of [^{14}C]PAH by hOAT1 in a concentration-dependent manner (Fig. 2A). The estimated IC_{50} values of famotidine for these three transporters were higher than those of cimetidine.

3.2. Transport of famotidine and cimetidine by hOAT1, hOAT3 and hOCT2

Famotidine transport by hOAT1, hOAT3 or hOCT2 was examined using Xenopus oocyte expression system. As shown in Fig. 3, famotidine uptake into the hOAT3-expressing oocytes significantly exceeded that into water-injected oocytes. Estrone sulfate completely inhibited the famotidine uptake to the level of water-injected oocytes. These findings indicate that famotidine is a substrate for hOAT3. In contrast to hOAT3, famotidine uptake values by hOAT1- and hOCT2-expressing oocytes were not different from those by water-injected oocytes (Figs. 4A and 5A). In addition, we evaluated the cimetidine uptake by hOAT1 and hOCT2 to compare with famotidine. As shown in Figs. 4B and 5B, injection of hOAT1 and hOCT2 cRNA in oocytes stimulated the cimetidine uptake. PAH or MPP reduced the cimetidine accumulation in hOAT1- or hOCT2-expressing oocytes to those of water-injected control, respectively.

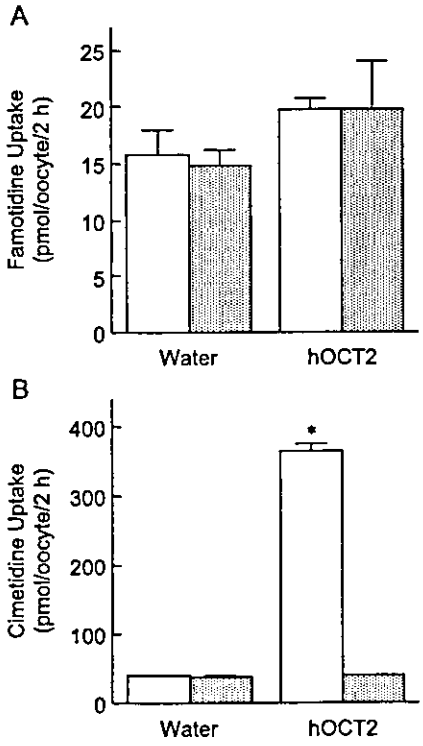

Fig. 5. Uptake of famotidine (A) and cimetidine (B) by hOCT2-expressing oocytes. Water-injected or hOCT2-expressing oocytes were incubated with famotidine or cimetidine at 1 mM in the absence (open column) or presence (dotted column) of 5 mM MPP for 2 h. Each column represents the mean±S.E.M. of five to eight measurements. Four oocytes were used for each uptake measurement. *$P<0.05$, significantly different from the other three columns.

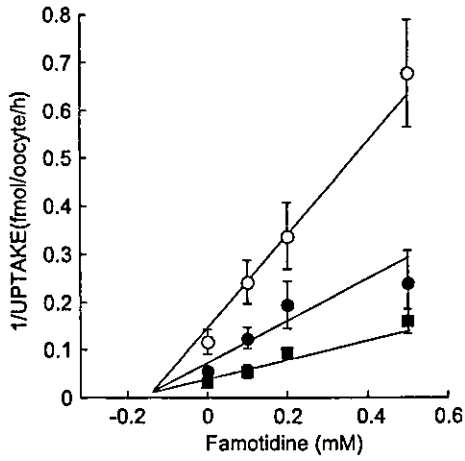

Fig. 6. Dixon plot for inhibitory effects of famotidine on [^{3}H]estrone sulfate uptake by hOAT3-expressing oocytes. hOAT3-expressing oocytes were incubated with [^{3}H]estrone sulfate (20 nM, ○; 40 nM, ●; 80 nM, ■) with famotidine at the indicated concentrations for 1 h. The levels of [^{3}H]estrone sulfate uptake was determined, and figures were drawn after subtraction of the uptake in water-injected oocytes from that in hOAT3 cRNA-injected oocytes. Values are represented as 1/uptake. Each point represents the mean±S.E.M. of 7 to 10 oocytes.

We performed Dixon plot analysis to determine the inhibitory mode of famotidine on the hOAT3 mediated estrone sulfate uptake, and the results were shown in Fig. 6. Famotidne inhibited competitively, and apparent Ki value was estimated to be 179±24 μM.

4. Discussion

In this study, we examined whether basolateral organic ion transporters such as hOAT1, hOAT3 and hOCT2 recognized famotidine as substrate in comparison with cimetidine. It was shown that there were marked differences between famotidine and cimetidine in the recognition and transport properties by renal organic ion transporters.

It was indicated that efficient tubular secretion contributed to renal excretion of famotidine and cimetidine in subjects with normal renal function. Inasmuch as these drugs are weak bases, it has been speculated that renal secretion of famotidine and cimetidine are mediated by the organic cation transporter. In the case of cimetidine, Urakami et al. (2001, 2002) demonstrated that the cimetidine was transported by rOCT2 and hOCT2, and similar results were obtained in this study (Fig. 5B). Furthermore, in 5/6 nephrectomized rats, renal clearance of cimetidine showed a significant correlation with rOCT2 expression levels in the kidney (Ji et al., 2002). Therefore, hOCT2 may contribute to the renal secretion of cimeti-

dine. Unexpectedly, hOCT2 did not show any famotidine transport (Fig. 5A). Due to the detection limit of HPLC analysis, the uptake experiments were performed at 1 mM. It is possible that saturation of the transporter make it difficult to detect the transport of famotidine by hOCT2. However, as expected and as opposed to famotidine, cimetidine transport by hOCT2 was detected. Arndt et al. (2001) reported that some organic cations, such as quinine and tetrapentylammonium, inhibited rOCT2 but that these compounds seemed to be not translocated via rOCT2. Therefore, it is likely that famotidine inhibits hOCT2 but is hardly transported by hOCT2 differently from cimetidine. Recently, Lee et al. (2002) reported that famotidine was not transported by the TEA-sensitive organic cation transport systems across the basolateral membrane in LLC-PK_1 cells. Inasmuch as LLC-PK_1 cells retain basolateral organic cation transporter of the kidney (Saito et al., 1992), the report of Lee et al. (2002) is consistent with our results. These data suggest that hOCT2 is involved in the basolateral transport of cimetidine but not of famotidine in the human kidney.

Recently, cimetidine was reported to be a substrate for hOAT1 and hOAT3 in addition to hOCT2 (Cha et al., 2001; Burckhardt et al., 2003), and our present results are consistent with these reports. Gisclon et al. (1989) reported that probenecid, a classic inhibitor of organic anion, decreased the renal clearance of cimetidine. It was implied that organic anion transporters were concerned with renal secretion of cimetidine. However, in the report of Gisclon et al. (1989), interaction between cimetidine and probenecid was transient and slight. Although further studies are needed to calculate the contribution of hOATs for cimetidine excretion, it is speculated that organic anion transporters play minor roles for renal secretion of cimetidine. On the other hand, Inotsume et al. (1990) reported that probenecid had a pronounced effect on renal tubular secretion of famotidine. The tubular secretory clearance of famotidine was decreased to one-tenth by coadministration of probenecid. As probenecid is well known as a potent inhibitor for hOAT3, their report is consistent with our present results that hOAT3, but not hOCT2, mediated famotidine uptake. Therefore, it is suggested that hOCT2 plays one of the important roles for renal uptake of cimetidine and hOAT3 for famotidine uptake, respectively.

Dowling et al. (2001) showed that tubular secretion of famotidine in human was not saturated at its unbound plasma concentrations up to about 10 μM. In the present study, the estimated Ki value of famotidine for hOAT3 was 179 μM (Fig. 6), suggesting that the famotidine transport by hOAT3 was not saturated at the therapeutic levels. Boom et al. (1996) reported that the apparent Michaelis–Menten constant (K_T) for tubular secretion of famotidine in vivo was 76 μM using the beagle dog. The K_T value in the report of Boom et al. is lower than the Ki value of famotidine for hOAT3 (179 μM) in this study. At present, it is difficult to discuss the difference between the K_T value of Boom et al. and our Ki value because of various factors such as species difference and experimental conditions.

It is well known that cimetidine reduces the renal secretion of procainamide (Somogyi et al., 1983), although famotidine had no effect on the pharmacokinetics of procainamide (Klotz et al., 1985). In this study, we assessed the inhibitory potency of cimetidine on hOCT2, the candidate responsible for the renal uptake of procainamide. The IC_{50} of the cimetidine for hOCT2 was around its therapeutic plasma concentration. Therefore, cimetidine may block the hOCT2 transport activity in vivo. On the other hand, the inhibitory potency of famotidine for hOCT2 was weaker than that of cimetidine, and the clinical plasma levels of famotidine (0.15±0.06 μM; Yoshimoto et al., 1994) were extremely lower than the IC_{50} for hOCT2. Therefore, famotidine cannot inhibit hOCT2 transport in the kidney at the therapeutic dose. In this study, the IC_{50} of famotidine for hOAT3 was also much higher than the clinical plasma concentration, and famotidine did not interact with hOAT1. Differently from cimetidine, famotidine is not likely to inhibit the tubular secretion of other drugs via these organic ion transporters, hOAT1, hOAT3 and hOCT2.

Several reports represented that pharmacokinetics of famotidine was related with renal function (Takabatake et al., 1985; Lin et al., 1988). Dosage adjustment of famotidine is necessary for the patients with renal insufficiency. In our previous studies, expression levels of renal drug transporters were altered in the impaired kidney. The expression level of rOCT2 was decreased in the 5/6 nephrectomized rats, but those of rOAT1, rOAT3 and rOCT1 were not influenced (Ji et al., 2002). Hyperuricemic rats represented the down-regulation of rOAT1, rOAT3 and rOCT2 but not of rOCT1 (Habu et al., 2003). Recently, we reported the alteration of organic ion transporters in the kidney of renal disease patients (Sakurai et al., 2004). In that report, elimination rate of cefazolin, which is substrate for hOAT3, was correlated with hOAT3 mRNA level, suggesting that the expression levels of renal drug transporter affect urinary drug excretion. It is interesting whether renal excretion of famotidine is affected by hOAT3 expression level in the patients with renal insufficiency.

In conclusion, this study represented the differences between famotidine and cimetidine in the interaction with human renal organic ion transporters, hOAT1, hOAT3 and hOCT2, and suggested that hOAT3 contributed to the renal tubular secretion of famotidine. Theses findings could be useful information to understand the renal handling of famotidine and to make optimum dosage regimens of the histamine H_2 receptor antagonists.

Acknowledgements

This study was supported by a grant-in-aid for Comprehensive Research on Aging and Health from the Ministry of

Health, Labor, and Welfare of Japan, by a grant-in-aid for Scientific Research from the Ministry of Education, Culture, Sports, Science, and Technology of Japan, and by 21st Century COE Program "Knowledge Information Infrastructure for Genome Science."

References

Arndt, P., Volk, C., Gorboulev, V., Budiman, T., Popp, C., Ulzheimer-Teuber, I., Akhoundova, A., Koppatz, S., Bamberg, E., Nagel, G., Koepsell, H., 2001. Interaction of cations, anions, and weak base quinine with rat renal cation transporter rOCT2 compared with rOCT1. Am. J. Physiol. Renal. Physiol. 281, F454–F468.

Boom, P.A., Hoet, S., Russel, F.G.M., 1996. Saturable urinary excretion kinetics of famotidine in the dog. J. Pharm. Pharmacol. 49, 288–292.

Burckhardt, B.C., Brai, S., Wallis, S., Krick, W., Wolff, N.A., Burckhardt, G., 2003. Transport of cimetidine by flounder and human renal organic anion transporter 1. Am. J. Physiol. Renal. Physiol. 284, F503–F509.

Cha, S.H., Sekine, T., Fukushima, J., Kanai, Y., Kobayashi, Y., Goya, T., Endou, H., 2001. Identification and characterization of human organic anion transporter 3 expressing predominantly in the kidney. Mol. Pharmacol. 59, 1277–1286.

Christian Jr., C.D., Meredith, C.G., Speeg Jr., K.V., 1984. Cimetidine inhibits renal procainamide clearance. Clin. Pharmacol. Ther. 36, 221–227.

Dowling, T.C., Frye, R.F., Fraley, D.S., Matzke, G.R., 2001. Characterization of tubular functional capacity in humans using *para*-aminohippurate and famotidine. Kidney Int. 59, 295–303.

Dresser, M.J., Leabman, M.K., Giacomini, K.M., 2001. Transporters involved in the elimination of drugs in the kidney: organic anion transporters and organic cation transporters. J. Pharm. Sci. 90, 397–421.

Gisclon, L.G., Boyd, R.A., Williams, R.L., Giacomini, K.M., 1989. The effect of probenecid on the renal elimination of cimetidine. Clin. Pharmacol. Ther. 45, 444–452.

Habu, Y., Yano, I., Takeuchi, A., Saito, H., Okuda, M., Fukatsu, A., Inui, K., 2003. Decreased activity of basolateral organic ion transports in hyperuricemic rat kidney: roles of organic ion transporters, rOAT1, rOAT3 and rOCT2. Biochem. Pharmacol. 66, 1107–1114.

Howard, J.M., Chremos, A.N., Collen, M.J., McArthur, K.E., Cherner, J.A., Maton, P.N., Ciarleglio, C.A., Cornelius, M.J., Gardner, J.D., Jensen, R.T., 1985. Famotidine, a new, potent, long-acting histamine H_2-receptor antagonist: comparison with cimetidine and ranitidine in the treatment of Zollinger-Ellison syndrome. Gastroenterology 88, 1026–1033.

Humphries, T.J., 1987. Famotidine: a notable lack of drug interactions. Scand. J. Gastroenterol. 22, 55–60.

Inotsume, N., Nishimura, M., Nakano, M., Fujiyama, S., Sato, T., 1990. The inhibitory effect of probenecid on renal excretion of famotidine in young, healthy volunteers. J. Clin. Pharmacol. 30, 50–56.

Inui, K., Masuda, S., Saito, H., 2000. Cellular and molecular aspects of drug transport in the kidney. Kidney Int. 58, 944–958.

Ji, L., Masuda, S., Saito, H., Inui, K., 2002. Down-regulation of rat organic cation transporter rOCT2 by 5/6 nephrectomy. Kidney Int. 62, 514–524.

Klotz, U., Arvela, P., Rosenkranz, B., 1985. Famotidine, a new H_2-receptor antagonist, does not affect hepatic elimination of diazepam or tubular secretion of procainamide. Eur. J. Clin. Pharmacol. 28, 671–675.

Kusuhara, H., Sekine, T., Utsunomiya-Tate, N., Tsuda, M., Kojima, R., Cha, S.H., Sugiyama, Y., Kanai, Y., Endou, H., 1999. Molecular cloning and characterization of a new multispecific organic anion transporter from rat brain. J. Biol. Chem. 274, 13675–13680.

Lee, K., Ng, C., Brouwer, K.L., Thakker, D.R., 2002. Secretory transport of ranitidine and famotidine across Caco-2 cell monolayers. J. Pharmacol. Exp. Ther. 303, 574–580.

Lin, J.H., Chremos, A.N., Yeh, K.C., Antonello, J., Hessey II, G.A., 1988. Effects of age and chronic renal failure on the urinary excretion kinetics of famotidine in man. Eur. J. Clin. Pharmacol. 34, 41–46.

Motohashi, H., Sakurai, Y., Saito, H., Masuda, S., Urakami, Y., Goto, M., Fukatsu, A., Ogawa, O., Inui, K., 2002. Gene expression levels and immunolocalization of organic ion transporters in the human kidney. J. Am. Soc. Nephrol. 13, 866–874.

Saito, H., Yamamoto, M., Inui, K., Hori, R., 1992. Transcellular transport of organic cation across monolayers of kidney epithelial cell line LLC-PK_1. Am. J. Physiol. 262, C59–C66.

Sakurai, Y., Motohashi, H., Ueo, H., Masuda, S., Saito, H., Okuda, M., Mori, N., Matsuura, M., Doi, T., Fukatsu, A., Ogawa, O., Inui, K., 2004. Expression levels of renal organic anion transporters (OATs) and their correlation with anionic drug excretion in patients with renal diseases. Pharm. Res. 21, 61–67.

Sekine, T., Cha, S.H., Endou, H., 2000. The multispecific organic anion transporter (OAT) family. Pflügers Arch. 440, 337–350.

Somogyi, A., McLean, A., Heinzow, B., 1983. Cimetidine–procainamide pharmacokinetic interaction in man: evidence of competition for tubular secretion of basic drugs. Eur. J. Clin. Pharmacol. 25, 339–345.

Takabatake, T., Ohta, H., Maekawa, M., Yamamoto, Y., Ishida, Y., Hara, H., Nakamura, S., Ushiogi, Y., Kawabata, M., Hashimoto, N., Hattori, N., 1985. Pharmacokinetics of famotidine, a new H_2-receptor antagonist, in relation to renal function. Eur. J. Clin. Pharmacol. 28, 327–331.

Urakami, Y., Okuda, M., Masuda, S., Akazawa, M., Saito, H., Inui, K., 2001. Distinct characteristics of organic cation transporters, OCT1 and OCT2, in the basolateral membrane of renal tubules. Pharm. Res. 18, 1528–1534.

Urakami, Y., Akazawa, M., Saito, H., Okuda, M., Inui, K., 2002. cDNA cloning, functional characterization, and tissue distribution of an alternatively spliced variant of organic cation transporter hOCT2 predominantly expressed in the human kidney. J. Am. Soc. Nephrol. 13, 1703–1710.

Uwai, Y., Saito, H., Hashimoto, Y., Inui, K., 2000. Interaction and transport of thiazide diuretics, loop diuretics, and acetazolamide via rat renal organic anion transporter rOAT1. J. Pharmacol. Exp. Ther. 295, 261–265.

van Crugten, J., Bochner, F., Keal, J., Somogyi, A., 1986. Selectivity of the cimetidine-induced alterations in the renal handling of organic substrates in humans. Studies with anionic, cationic and zwitterionic drugs. J. Pharmacol. Exp. Ther. 236, 481–487.

Wade, E., Rebuck, J., Healey, M., Rogers, F., 2002. H_2 antagonist-induced thrombocytopenia: is this a real phenomenon? Intensive Care Med. 28, 459–465.

Yoshimoto, K., Saima, S., Echizen, H., Nakamura, Y., Kondo, T., Yagishita, Y., Ishizaki, T., 1994. Famotidine-associated central nervous system reactions and plasma and cerebrospinal drug concentrations in neurosurgical patients with renal failure. Clin. Pharmacol. Ther. 55, 693–700.

Pharmaceutical Research, Vol. 22, No. 2, February 2005 (© 2005)
DOI: 10.1007/s11095-004-1193-3

Research Paper

Metformin Transport by Renal Basolateral Organic Cation Transporter hOCT2

Naoko Kimura,[1] Masahiro Okuda,[1] and Ken-ichi Inui[1,2]

Received September 2, 2004; accepted October 22, 2004

Purpose. Metformin, an antihyperglycemic agent, is eliminated by tubular secretion in addition to glomerular filtration in the human kidney. This study was performed to characterize metformin transport by human organic cation transporter 2 (hOCT2), the most abundant organic cation transporter in the basolateral membranes of the human kidney.
Methods. Accumulation of [^{14}C]metformin was assessed by the tracer experiments in the human embryonic kidney (HEK293) cells expressing hOCT2.
Results. The transport of [^{14}C]metformin was markedly stimulated in hOCT2-expressing cells compared with the vector-transfected cells. The accumulation of [^{14}C]metformin was concentrative and was dependent on the membrane potential, showing consistency with the characteristics of hOCT2. The apparent K_m and V_{max} values of [^{14}C]metformin transport by hOCT2-expressing HEK293 cells were 1.38 ± 0.21 mM and 11.9 ± 1.5 nmol mg protein^{-1} min^{-1}, respectively. The order of the potencies of unlabeled biguanides to inhibit [^{14}C]metformin transport by hOCT2 was phenformin > buformin > metformin. Furthermore, [^{14}C]metformin transport was inhibited slightly or moderately by cationic drugs such as procainamide and quinidine at respective therapeutic concentrations.
Conclusions. Metformin is transported by the basolateral organic cation transporter hOCT2 in the human kidney. hOCT2 could play a role in the drug interactions between metformin and some cationic drugs.

KEY WORDS: hOCT2; human kidney; metformin; organic cation transporter; renal tubular secretion.

INTRODUCTION

Biguanide agents have been used for the treatment of type 2 diabetes mellitus since the late 1950s. These drugs are useful in primary therapy for type 2 diabetes mellitus with obesity or hyperlipidemia and can also be used for add-on therapy in patients with diabetes uncontrolled by sulfonylureas and diet (1–2). The mechanisms of the pharmacological action of metformin involve the decreased hepatic glucose production without an effect on the release of insulin and the increased glycogenesis and lactate production. The most life-threatening adverse effect of biguanides is lactic acidosis, because there is a risk of overproduction of lactate through inhibition of mitochondrial respiration and increased anaerobic glycolysis (1). A risk of decreased use of lactate through inhibition of gluconeogenesis by biguanides has been also documented (1). Although phenformin was removed from the market because of its association with lactic acidosis, the relative risk is much lower for metformin than for phenformin. Moreover, the risk of lactic acidosis caused by metformin is less than the risk of severe hypoglycemia induced by sulfonylurea drugs (3).

Metformin is mainly excreted into urine, almost entirely in an unchanged form. The renal clearance of metformin (440–454 ml/min) is much higher than the glomerular filtration rate in humans (4–5), suggesting a significant contribution of tubular secretion in addition to glomerular filtration. As biguanides consist of two molecules of guanidine linked together by the removal of an ammonia group, they are protonated at physiologic pH. Organic cation transporters have been suggested to mediate tubular secretion of metformin (6–7); however, the molecular mechanisms underlying the renal tubular secretion of biguanides have not been clarified.

Organic cation transporters in the kidney, liver, intestine, brain, and placenta play essential physiologic and pharmacological roles in the handling of cationic drugs and endogenous organic ions. Human organic cation transporter 1 (hOCT1) is expressed primarily in the liver (8–9) and is likely responsible for the hepatic uptake of various cationic drugs. In contrast to hOCT1, we demonstrated that human organic cation transporter 2 (hOCT2) is the most abundant organic cation transporter in the basolateral membranes of human kidney (10). Moreover, hOCT2 as well as its orthologue in the rat (rOCT2) were localized at the basolateral membranes of renal proximal tubules and were suggested to contribute to the secretion of organic cations, such as tetraethylammonium,

[1] Department of Pharmacy, Kyoto University Hospital, Kyoto University, Kyoto 606-8507, Japan.
[2] To whom correspondence should be addressed. (E-mail: inui@kuhp.kyoto-u.ac.jp)

ABBREVIATIONS: hOCT1, human organic cation transporter 1; hOCT2, human organic cation transporter 2; rOCT1, rat organic cation transporter 1; HEPES, *N*-2-hydroxyethylpiperazine-*N*′-2-ethanesulfonic acid.

0724-8741/05/0200-0255/0 © 2005 Springer Science+Business Media, Inc.

1-methyl-4-phenylpyridinium, cimetidine, and guanidine (10–13). Recently, rat (r) OCT1 as well as mouse (m) OCT1 was revealed to transport biguanides (14,15). It was also demonstrated that tissue distribution of metformin was decreased in the liver, duodenum, jejunum, ileum, but not in the kidney and colon, in the mOCT1 gene-knockout mice. Moreover, Dresser *et al.* (16) reported that metformin and phenformin induced currents and *trans*-stimulated [^{3}H]1-methyl-4-phenylpyridinium uptake in *Xenopus* oocytes expressing hOCT1 and hOCT2. However, information has been limited regarding the characteristics of metformin transport by hOCT2 and hOCT2-mediated drug interactions between metformin and concomitantly administered drugs. In the current study, we characterized the transport of [^{14}C]metformin using human embryonic kidney (HEK293) cells stably expressing hOCT2. We also assessed drug interactions between [^{14}C]metformin and various cationic drugs.

MATERIALS AND METHODS

Materials

[Biguanidine-^{14}C]metformin hydrochloride (26 mCi/mmol) was purchased from Moravek Biochemicals, Inc. (Brea, CA, USA). [Ethyl-1-^{14}C]tetraethylammonium bromide (55 mCi/mmol) was purchased from American Radiolabeled Chemicals (St. Louis, MO, USA). Metformin, phenformin, and 1-methyl-4-phenylpyridinium iodide were obtained from Sigma-Aldrich Co. (St. Louis, MO, USA). Buformin was purchased from Wako Pure Chemicals (Osaka, Japan). Tetraethylammonium bromide and cimetidine were obtained from Nacalai Tesque Inc. (Kyoto, Japan). All other compounds used were of the highest purity available.

Cell Culture and Transfection

To construct the transfectant stably expressing hOCT2, HEK 293 cells (ATCC CRL-1573, American Type Culture Collection, Manassas, VA, USA), a transformed cell line derived from human embryonic kidney, were transfected with 0.8 μg of total plasmid DNA (pCMV-XL4:pBK-CMV vector = 2:1) per well. At 24 h after transfection, the cells split between 1:15 and 1:30 were cultured in complete medium consisting of Dulbecco's modified Eagle's medium with 10% fetal bovine serum in an atmosphere of 5% CO_2/95% air at 37°C containing G418 (0.5 mg/ml) (Wako Pure Chemical Industries, Osaka, Japan). Then, 14 to 21 days after transfection, single colonies were selected. G418-resistant colonies were analyzed by RT-PCR for expression of hOCT2 mRNA (17).

For uptake experiments, the cells were seeded onto poly-D-lysine–coated 24-well plates at a density of 2.0×10^5 cells per well. The cell monolayers were used at day 3 of culture for uptake experiments. In this study, HEK293 cells between passages 70 and 83 were used.

Uptake Experiments

Cellular uptake of cationic compounds was measured with monolayer cultures of HEK293 cells grown on poly-D-lysine–coated 24-well plates (17). The incubation medium for uptake experiments contained 145 mM NaCl, 3 mM KCl, 1 mM $CaCl_2$, 0.5 mM $MgCl_2$, 5 mM D-glucose, and 5 mM HEPES (pH 7.4). The composition of the high K^+ incubation medium was 3 mM NaCl, 145 mM KCl, 1 mM $CaCl_2$, 0.5 mM $MgCl_2$, 5 mM D-glucose, and 5 mM HEPES (pH 7.4). When indicated, 9.2 mM $BaCl_2$ was added to the incubation medium. The pH of the medium was adjusted with NaOH or HCl. The cells were preincubated with 0.2 ml of incubation medium for 10 min at 37°C. The medium was then removed, and 0.2 ml of incubation medium containing [^{14}C]metformin or [^{14}C]tetraethylammonium was added. The medium was aspirated off at the end of the incubation, and the monolayers were rapidly rinsed twice with 1 ml of ice-cold incubation medium. The cells were solubilized in 0.5 ml of 0.5 N NaOH, and then the radioactivity in aliquots was determined by liquid scintillation counting. The protein content of the solubilized cells was determined by the method of Bradford (18), using a Bio-Rad Protein Assay Kit (Bio-Rad Laboratories, Hercules, CA, USA) with bovine γ-globulin as a standard. The concentration dependence of metformin transport by hOCT2 was analyzed using the Michaelis-Menten equation; $V = V_{max} \cdot [S]/(K_m + [S]) + K_d \cdot [S]$, where V is the transport rate, V_{max} is the maximum transport rate, [S] is the concentration of metformin, K_m is the Michaelis constant, and K_d is a diffusion constant. For the *cis*-inhibition study, the uptake of [^{14}C]metformin was achieved by adding various concentrations of unlabeled inhibitors to the incubation medium. The IC_{50} values were calculated from the inhibition plots based on the equation, $V = V_0/[1 + (I/IC_{50})^n]$ by nonlinear least square regression analysis with Kaleidagraph Version 3.5 (Synergy Software, Reading, PA, USA) (12). V and V_0 are the uptake rates of [^{14}C]metformin in the presence and absence of inhibitor, respectively. I is the concentration of inhibitor, and n is the Hill coefficient.

Statistical Analyses

Data were analyzed statistically by one-way analysis of variance followed by Dunnett's test. p values of less than 0.05 were considered to be significant.

RESULTS

Concentration Dependence of [^{14}C]Metformin Transport by hOCT2

To examine whether metformin is transported by hOCT2, we evaluated the uptake of [^{14}C]metformin by HEK293 cells stably expressing hOCT2. Figure 1 illustrates the time-course of [^{14}C]metformin uptake by HEK 293 cells transfected with hOCT2 and empty vector (Fig. 1). The uptake of [^{14}C]metformin increased time-dependently, and was linear for up to 2 min. Figure 2 shows the concentration dependence of [^{14}C]metformin uptake by hOCT2-expressing cells. The uptake of [^{14}C]metformin by these cells was saturated at high concentrations. The apparent Michaelis-Menten constant (K_m) value of [^{14}C]metformin uptake by hOCT2-transfected cells, estimated by subtracting the nonsaturable component of [^{14}C]metformin transport in the presence of 1-methyl-4-phenylpyridinium (5 mM) was 1.38 ± 0.21 mM. The maximal uptake rate (V_{max}) value of the [^{14}C]metformin uptake by hOCT2-transfected cells was 11.9 ± 1.5 nmol mg protein^{-1} min^{-1} (mean ± SE of three separate experiments using three monolayers).

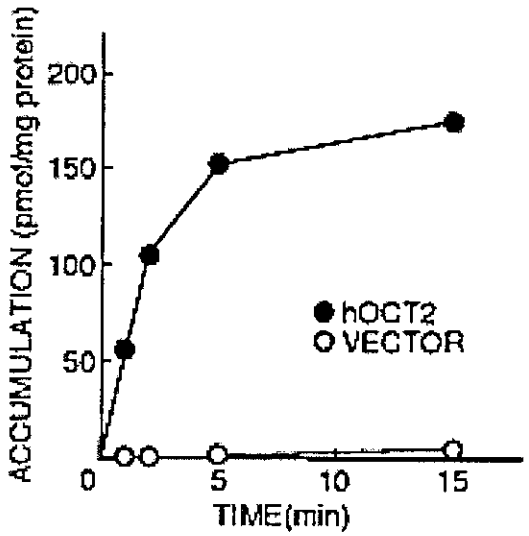

Fig. 1. Time course of [^{14}C]metformin uptake by HEK293 cells stably expressing hOCT2. HEK 293 cells transfected with hOCT2 (●) or pCMV6-XL4 vector (○) were incubated for the specified periods (1, 2, 5, and 15 min) at 37°C with 0.2 ml of 10 μM [^{14}C]metformin (pH 7.4). Each point represents the mean ± SE of three monolayers from a typical experiment.

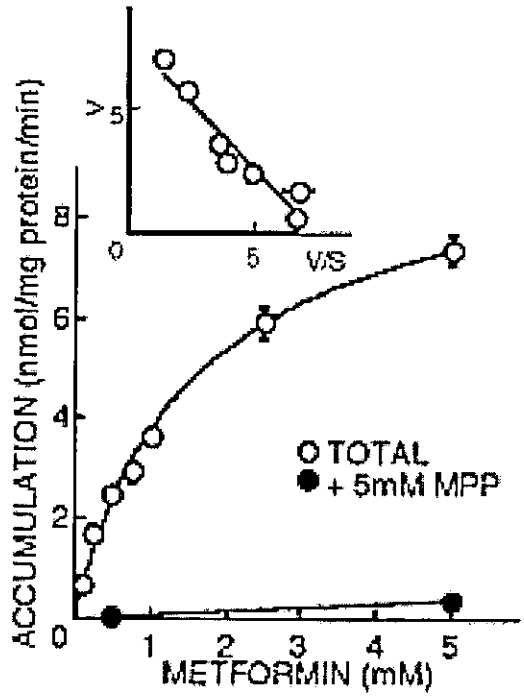

Fig. 2. Concentration dependence of [^{14}C]metformin transport by hOCT2. hOCT2 transfectants were incubated at 37°C for 2 min with various concentrations of [^{14}C]metformin (100, 250, 500, 750, 1000, 2500, and 5000 μM) in the absence (○) or presence (●) of 5 mM 1-methyl-4-phenylpyridinium (pH 7.4). Each point represents the mean ± SE of three monolayers from a typical experiment. Inset: Eadie-Hofstee plots of metformin uptake after correction for non-saturable components. V, uptake rate (nmol mg protein^{-1} min^{-1}); S, metformin concentration (mM).

Effect of Membrane Potential on the Transport of [^{14}C]Metformin and [^{14}C]Tetraethylammonium by hOCT2

Next, we examined the effect of membrane potential on the accumulation of [^{14}C]metformin and [^{14}C]tetraethylammonium in HEK293 cells expressing hOCT2 (Fig. 3). The accumulation of [^{14}C]metformin in hOCT2-expressing cells decreased in the presence of high K^+ (145 mM) medium (Fig. 3A) similarly as observed for [^{14}C]tetraethylammonium (Fig. 3B). Furthermore, the accumulation of [^{14}C]metformin and [^{14}C]tetraethylammonium *via* hOCT2 decreased in the presence of Ba^{2+} (9.2 mM), a nonselective blocker of K^+ channels. The mean percent of control values ± SE of [^{14}C]metformin accumulation obtained from three separate experiments using three monolayers were 24.8 ± 2.8% and 59.0 ± 9.9% for high K^+ and Ba^{2+} media, respectively ($p < 0.01$ vs. control). The values ± SE of [^{14}C]tetraethylammonium accumulation were 17.8 ± 2.7% and 39.7 ± 9.6% for high K^+ and Ba^{2+} media, respectively ($p < 0.01$ vs. control).

Inhibition of hOCT2-Mediated Transport of [^{14}C]Metformin by Cationic Drugs

To assess the potencies of cationic drugs to cause drug-interactions with hOCT2-mediated metformin transport, we examined the inhibitory effects of several cationic compounds on the uptake of [^{14}C]metformin by the hOCT2-expressing cells (Fig. 4). Then, we calculated the IC_{50} values of cationic compounds from the inhibition plots as described in "Materials and Methods." Tetraethylammonium (a typical substrate for the renal organic cation transporter), 1-methyl-4-phenylpyridinium (a cationic neurotoxin), procainamide and quinidine (antiarrhythmic drugs), trimethoprim (an antibiotic), and cimetidine and ranitidine (H_2 receptor antagonists) inhibited the uptake of [^{14}C]metformin by hOCT2-expressing cells in a dose-dependent manner. As summarized in Table I, 1-methyl-4-phenylpyridinium showed the most potent inhibitory effect, whereas procainamide and cimetidine had moderate inhibitory effects on the transport of metformin by hOCT2. Furthermore, biguanides inhibited the transport of [^{14}C]metformin by hOCT2 in the following order: phenformin > buformin > metformin.

DISCUSSION

In the current study, we characterized [^{14}C]metformin transport using hOCT2-expressing HEK293 cells, and assessed drug interactions between metformin and cationic drugs using [^{14}C]metformin as a tracer. [^{14}C]metformin uptake was markedly enhanced in HEK293 cells stably transfected with hOCT2 (Fig. 1). The uptake of [^{14}C]metformin was dependent on membrane potential (Fig. 3), being consistent with the functional characteristics of OCT2 (13,19). To our knowledge, this is the first demonstration showing direct evidence of metformin transport by hOCT2. Considering that hOCT2 is the dominant organic cation transporter expressed in the basolateral membranes of the human renal cortex (10), hOCT2 should play a relevant role in the transport of metformin across basolateral membranes in the human kidney.

The accumulation of [^{14}C]metformin in hOCT2-expressing cells was saturated at high concentrations (Fig. 2). Although the driving force of both compounds by hOCT2 seems to be common, that is, the membrane potential (Fig. 3), the apparent affinity of metformin to hOCT2 (K_m = 1.38 mM) was much lower than that of tetraethylammonium

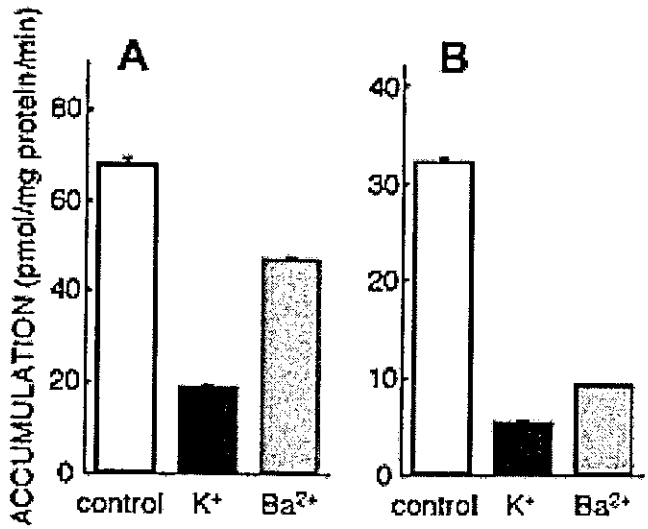

Fig. 3. Effect of membrane potential on [^{14}C]metformin (A) and [^{14}C]tetraethylammonium (B) transport by hOCT2. The cells transfected with hOCT2 were incubated with respective buffers at 37°C for 2 min with 10 μM [^{14}C]metformin (A) or 5 μM [^{14}C]tetraethylammonium (B) (pH 7.4). Each column represents the mean ± SE of three monolayers from a typical experiment.

(K_m = 431 μM) (13). Because the maximum plasma concentration of metformin was reported to be 9–12 μM after a single oral administration of metformin HCl (850 mg) in patients with type 2 diabetes mellitus (20–22) and up to 15 μM and 25 μM in healthy elderly patients and patients with moderate chronic renal impairment, respectively (23), the transport of metformin by hOCT2 should not saturate at therapeutic concentrations. Moreover, these results seem to be

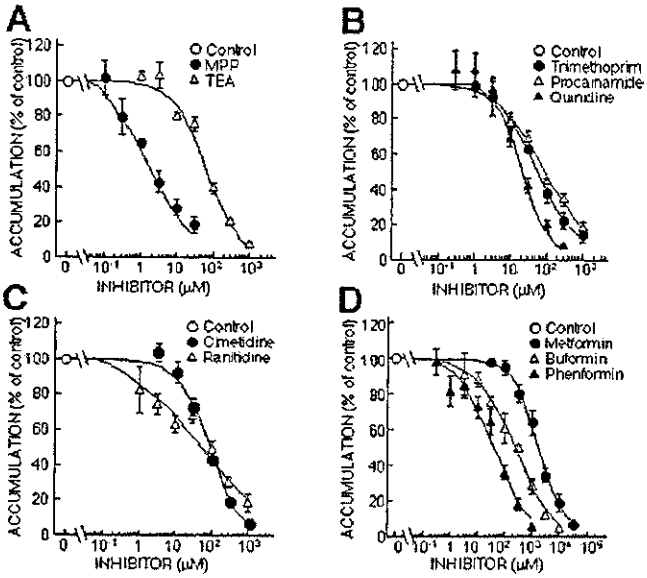

Fig. 4. Effects of cationic compounds on [^{14}C]metformin transport by hOCT2. HEK 293 cells transfected with hOCT2 were incubated at 37°C for 2 min with 10 μM [^{14}C]metformin (pH 7.4) in the presence of (A) 1-methyl-4-phenylpyridinium (MPP, ●) or tetraethylammonium (TEA, △); (B) trimethoprim (●), procainamide (△), or quinidine (▲); (C) cimetidine (●) or ranitidine (△); (D) metformin (●), buformin (△), or phenformin (▲). Each point represents the mean ± SE of three to six separate experiments using three monolayers.

Table I. The Apparent IC_{50} Values of Various Cationic Compounds for [^{14}C]Metformin Uptake by hOCT2

Compounds	Apparent IC_{50} values for [^{14}C]metformin uptake (μM)
MPP	2.99 ± 1.15
Quinidine	17.4 ± 5.7
Phenformin	55.3 ± 12.5
Trimethoprim	60.0 ± 19.0
TEA	66.6 ± 2.3
Cimetidine	72.6 ± 11.4
Ranitidine	74.6 ± 32.2
Procainamide	79.8 ± 7.5
Buformin	203 ± 63
Metformin	1840 ± 370

See experimental conditions in the legend of Fig. 4. The apparent IC_{50} values were calculated from inhibition plots (Fig. 4) by nonlinear regression analysis as described in "Materials and Methods." The data represent the mean ± SE of three to six separate experiments using three monolayers. MPP, 1-methyl-4-phenylpyridinium; TEA, tetraethylammonium.

comparable with the reports by Sambol *et al.* (20) that renal clearance of metformin was not changed by single dosings between 850 mg and 2550 mg, respectively.

In the current study, we demonstrated the inhibition of hOCT2-mediated [^{14}C]metformin transport by various cationic drugs, and then calculated respective IC_{50} values (Fig. 4 and Table I). Of the organic cations tested, quinidine or procainamide inhibited [^{14}C]metformin transport with IC_{50} values of 17.4 μM and 79.8 μM, respectively, which were comparable to the plasma concentrations of these drugs. It is reported that the plasma concentration of *N*-acetylprocainamide, a major metabolite of procainamide, also inhibit renal organic cation transporters (24). Moreover, the plasma procainamide concentration was elevated, when the drug was administered concomitantly with cimetidine (25). Therefore, we consider that concomitant administration of quinidine or procainamide with metformin should decrease the tubular secretion of metformin by interrupting hOCT2.

Somogyi *et al.* (7) reported the presence of drug interactions between metformin and cimetidine, where renal clearance of metformin was reduced by cimetidine, while cimetidine disposition was not altered by concomitantly administered metformin. According to the fact that apparent K_m value of metformin transport by hOCT2 was about 10-fold larger than that of cimetidine (K_m = 145 μM, unpublished observation), it seems to be reasonable that renal disposition of metformin, but not of cimetidine, was decreased by the drug interaction between these drugs. Dresser *et al.* (16) reported that IC_{50} value of metformin on hOCT2-mediated [^{3}H]cimetidine transport was 1700 μM. Because the value was approximately 100-fold higher than the therapeutic concentration of metformin, we consider that their results may indicate the unchanged disposition of cimetidine by concomitant administration of metformin, which was observed by Somogyi *et al.* (7).

The transport of [^{14}C]metformin was inhibited dose-dependently by cimetidine. This phenomenon apparently seems to be comparable to the observation by Somogyi *et al.* (7) that cimetidine inhibited the tubular secretion of metformin, and thereby increased its plasma concentration. The IC_{50} value of cimetidine for metformin transport (72.6 ± 11.4 μM)

was moderately higher than the plasma concentration of cimetidine, i.e., a single oral dose of 200 mg of cimetidine to the patients with normal renal function gave C_{max} values of between 2.3 μM and 6.8 μM (26). These data suggest that contribution of hOCT2 in the drug interaction between metformin and cimetidine would be minimum. However, it is known that systemic clearance of cimetidine decreases in the patients with renal dysfunction (27) and in the elderly (28), and thereby increases plasma concentrations of cimetidine. Therefore, the role of hOCT2 in the drug interactions between metformin and cimetidine could be relatively large in the patients with decreased renal function.

In the current study, the order of the potencies of biguanides to inhibit [^{14}C]metformin transport was phenformin > buformin > metformin. Dresser *et al.* (16) also demonstrated that the potency of phenformin to inhibit [^{3}H]cimetidine transport by hOCT2 was higher than that of metformin, suggesting consistency with the data in the present study. Interestingly, Wang *et al.* (14,15) also reported the order of affinity of biguanides to the rOCT1 was phenformin > buformin > metformin, suggesting similar substrate spectrum between OCT1 and OCT2. This phenomenon seems to be reasonable, because substrate spectrums were similar between OCT1 and OCT2 as demonstrated by us (11,12). Because the information regarding the relationship between plasma concentration of biguanides and blood lactose levels is limited (21), the role of hOCT2 in the biguanides-induced lactic acidosis should be clarified in subsequent studies.

In conclusion, hOCT2 is involved in the basolateral membrane transport of metformin in the human kidney. hOCT2 could also play a relevant role in the drug interaction between metformin and some cationic drugs.

ACKNOWLEDGMENTS

This work was supported in part by a grant-in-aid for Comprehensive Research on Aging and Health from the Ministry of Health, Labor and Welfare of Japan, by a grant-in-aid for Scientific Research from the Ministry of Education, Science, Culture and Sports of Japan, and by the 21st Century COE program "Knowledge Information Infrastructure for Genome Science."

REFERENCES

1. P. Marchetti, R. Giannarelli, A. di Carlo, and R. Navalesi. Pharmacokinetic optimisation of oral hypoglycaemic therapy. *Clin. Pharmacokinet.* **21**:308–317 (1991).
2. T. B. Klepser and M. W. Kelly. Metformin hydrochloride: An antihyperglycemic agent. *Am. J. Health Syst. Pharm.* **54**:893–903 (1997).
3. I. W. Campbell. Metformin and the sulphonylureas: The comparative risk. *Horm. Metab. Res. Suppl.* **15**:105–111 (1985).
4. C. R. Sirtori, G. Franceschini, M. Galli-Kienle, G. Cighetti, G. Galli, A. Bondioli, and F. Conti. Disposition of metformin (N,N-dimethylbiguanide) in man. *Clin. Pharmacol. Ther.* **24**:683–693 (1978).
5. P. J. Pentikäinen, P. J. Neuvonen, and A. Penttilä. Pharmacokinetics of metformin after intravenous and oral administration to man. *Eur. J. Clin. Pharmacol.* **16**:195–202 (1979).
6. A. Somogyi and M. Muirhead. Pharmacokinetic interactions of cimetidine 1987. *Clin. Pharmacokinet.* **12**:321–366 (1987).
7. A. Somogyi, C. Stockley, J. Keal, P. Rolan, and F. Bochner. Reduction of metformin renal tubular secretion by cimetidine in man. *Br. J. Clin. Pharmacol.* **23**:545–551 (1987).
8. V. Gorboulev, J. C. Ulzheimer, A. Akhoundova, I. Ulzheimer-Teuber, U. Karbach, S. Quester, C. Baumann, F. Lang, A. E. Busch, and H. Koepsell. Cloning and characterization of two human polyspecific organic cation transporters. *DNA Cell Biol.* **16**: 871–881 (1997).
9. L. Zhang, M. J. Dresser, A. T. Gray, S. C. Yost, S. Terashita, and K. M. Giacomini. Cloning and functional expression of a human liver organic cation transporter. *Mol. Pharmacol.* **51**:913–921 (1997).
10. H. Motohashi, Y. Sakurai, H. Saito, S. Masuda, Y. Urakami, M. Goto, A. Fukatsu, O. Ogawa, and K. Inui. Gene expression levels and immunolocalization of organic ion transporters in the human kidney. *J. Am. Soc. Nephrol.* **13**:866–874 (2002).
11. Y. Urakami, M. Okuda, S. Masuda, H. Saito, and K. Inui. Functional characteristics and membrane localization of rat multispecific organic cation transporters, OCT1 and OCT2, mediating tubular secretion of cationic drugs. *J. Pharmacol. Exp. Ther.* **287**: 800–805 (1998).
12. Y. Urakami, M. Okuda, S. Masuda, M. Akazawa, H. Saito, and K. Inui. Distinct characteristics of organic cation transporters, OCT1 and OCT2, in the basolateral membrane of renal tubules. *Pharm. Res.* **18**:1528–1534 (2001).
13. Y. Urakami, M. Akazawa, H. Saito, M. Okuda, and K. Inui. cDNA cloning, functional characterization, and tissue distribution of an alternatively spliced variant of organic cation transporter hOCT2 predominantly expressed in the human kidney. *J. Am. Soc. Nephrol.* **13**:1703–1710 (2002).
14. D. S. Wang, J. W. Jonker, Y. Kato, H. Kusuhara, A. H. Schinkel, and Y. Sugiyama. Involvement of organic cation transporter 1 in hepatic and intestinal distribution of metformin. *J. Pharmacol. Exp. Ther.* **302**:510–515 (2002).
15. D. S. Wang, H. Kusuhara, Y. Kato, J. W. Jonker, A. H. Schinkel, and Y. Sugiyama. Involvement of organic cation transporter 1 in the lactic acidosis caused by metformin. *Mol. Pharmacol.* **63**:844–848 (2003).
16. M. J. Dresser, G. Xiao, M. K. Leabman, A. T. Gray, and K. M. Giacomini. Interactions of n-tetraalkylammonium compounds and biguanides with a human renal organic cation transporter (hOCT2). *Pharm. Res.* **19**:1244–1247 (2002).
17. Y. Urakami, N. Kimura, M. Okuda, and K. Inui. Creatinine transport by basolateral organic cation transporter hOCT2 in the human kidney. *Pharm. Res.* **21**:976–981 (2004).
18. M. M. Bradford. A Rapid and sensitive method for the quantitation of microgram quantities of protein utilizing the principle of protein-dye binding. *Anal. Biochem.* **72**:248–254 (1976).
19. M. Okuda, H. Saito, Y. Urakami, M. Takano, and K. Inui. cDNA cloning and functional expression of a novel rat kidney organic cation transporter, OCT2. *Biochem. Biophys. Res. Commun.* **224**: 500–507 (1996).
20. N. C. Sambol, J. Chiang, M. O'Conner, C. Y. Liu, E. T. Lin, A. M. Goodman, L. Z. Benet, and J. H. Karam. Pharmacokinetics and pharmacodynamics of metformin in healthy subjects and patients with noninsulin-dependent diabetes mellitus. *J. Clin. Pharmacol.* **36**:1012–1021 (1996).
21. A. J. Scheen. Clinical pharmacokinetics of metformin. *Clin. Pharmacokinet.* **30**:359–371 (1996).
22. M. B. Davidson and A. L. Peters. An overview of metformin in the treatment of type 2 diabetes mellitus. *Am. J. Med.* **102**:99–110 (1997).
23. N. C. Sambol, J. Chiang, E. T. Lin, A. M. Goodman, C. Y. Liu, L. Z. Benet, and M. G. Cogan. Kidney function and age are both predictors of pharmacokinetics of metformin. *J. Clin. Pharmacol.* **35**:1094–1102 (1995).
24. T. Katsura, M. Takano, Y. Tomita, M. Yasuhara, K. Inui, and R. Hori. Characteristics of organic cation transporter in rat renal basolateral membrane. *Biochim. Biophys. Acta* **1146**:197–202 (1993).
25. A. Somogyi, A. McLean, and B. Heinzow. Cimetidine-procainamide pharmacokinetic interaction in man: Evidence of competition for tubular secretion of basic drugs. *Eur. J. Clin. Pharmacol.* **25**:339–345 (1983).
26. R. Larsson, G. Bodemar, and B. Norlander. Oral absorption of cimetidine and its clearance in patients with renal failure. *Eur. J. Clin. Pharmacol.* **15**:153–157 (1979).
27. P. A. Bjaeldager, J. B. Jensen, N. E. Larsen, and E. F. Hvidberg. Elimination of oral cimetidine in chronic renal failure and during haemodialysis. *Br. J. Clin. Pharmacol.* **9**:585–592 (1980).
28. A. Somogyi, H. G. Rohner, and R. Gugler. Pharmacokinetics and bioavailability of cimetidine in gastric and duodenal ulcer patients. *Clin. Pharmacokinet.* **5**:84–94 (1980).